Ψ_k **Scientific Highlight Of The Month**

No. 156 **February 2024**

Understanding metal bonding

Volker Heine[1,*], Siyu Chen[1,†]

[1] *TCM Group, Cavendish Laboratory, JJ Thomson Ave, Cambridge CB3 0HE, UK*

Abstract

This theoretical discussion covers several effects of metallic bonding based on a simple formula. It comes from the first steps in the Moment Method for calculating the local electronic structure of a solid (such as at a surface or in a random alloy), and depends on the square root of the total coordination number C of near neighbours. Each atom is covalently bonded to its cluster of near neighbours *as a whole*. The properties of metals touched on include malleability, crystal structure and phase transitions, vacancy formation energy, surface catalysis, surface reconstruction, graphite stability, and some aspects of the benzene molecule seen as an atomic metal ring. In most of these, the 'saturation' type of curvature of the square root function plays a crucial role. A short historical survey indicates the development of the ideas from Bloch (1929) to recent times.

Keywords: metals, malleable, metallic bonding, electronic structure.

This Ψ_k Scientific Highlight has been submitted as "Opinion Piece" to J. Phys. Condens. Matter.

---

[*] vh200@cam.ac.uk

[†] sc2090@cam.ac.uk

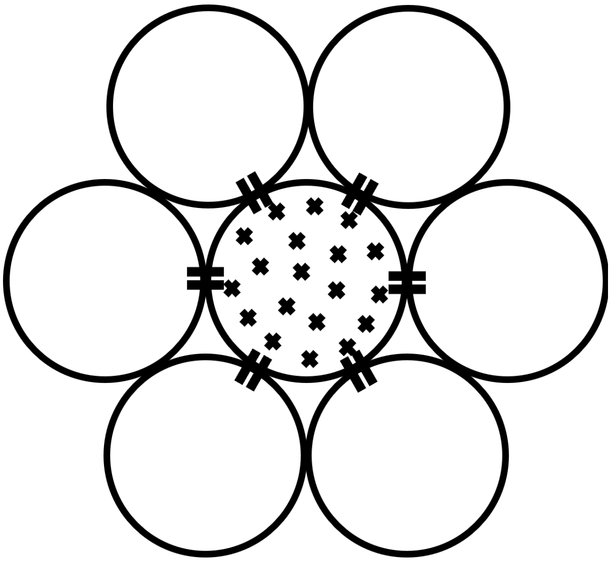

“Cluster” covalent bond to the whole cluster of C atoms
Strength $\propto \sqrt{C}$

$\Rightarrow$ crystal structures, phase transitions, strong but malleable, structure of defects, surface structure, surface catalysis, benzene molecule as atomic metallic ring, history.

Its mathematical logic builds on and connects steps in physics and chemistry from the earliest quantum ideas to now.

1 Bonding with a cluster of surrounding atoms as a whole

A characteristic property of metals is that they are malleable, and pure well-annealed samples can be very soft indeed. The paradox is that metallic bonds are usually strong, i.e. metals have strong cohesive energy: think of the force needed to break a steel bar. Perhaps understanding metallic bonding is best approached from the other characteristic metallic property, namely being good conductors of electricity (and heat, also carried by the electrons). In a well purified and annealed metal the accelerated electrons travel freely for tens of atomic diameters before being scattered by the thermal vibration of the atoms or perhaps by a defect.

Bonding between neighbouring atoms is a quantum mechanical effect, and the long mean free paths in electrical conduction show that one must think of the bonding electrons in metals delocalised in molecular orbitals extending throughout a specimen viewed as a vast molecule. In a crystalline solid the electrons are generally described as Bloch functions $\psi_{\mathbf{k}}$ with wave vector $\mathbf{k}$ and the phase factor $\exp(i\mathbf{k}\cdot\mathbf{r}_l)$ between atoms a distance $\mathbf{r}_l$ apart (Bloch 1929). Bloch's formulation of the $\psi_{\mathbf{k}}$ and the energies $E(\mathbf{k})$ of the electrons was to transfer to a crystal what had already been done for the wave functions in the hydrogen molecule (Heitler and London 1927), as he himself explained.*

Although the Bloch orbitals extend throughout the whole crystal, locally between neighbouring atoms they show a bonding and anti-bonding shape (Mott and Jones 1936) the same as seen throughout molecular chemistry (Pauling 1938). Thus figure 1 shows the first computed Bloch orbital by Wigner and Seitz (1933) with $\mathbf{k} = 0$ for metallic sodium. We note that it has the form of an atomic $3s$ electron inside the region of the Na^+ ionic core, and that there is a flat overlapping form half-way to the next atom as in the bonding orbital of the hydrogen molecule. For a more modern general reference, see Ashcroft and Mermin 1976.

Let us be a little more precise. Figure 1 shows the computed spherically symmetric wave function at an energy E_o giving zero gradient at the atomic radius R_a which is defined as the radius of the sphere with the same volume per atom of the crystal structure of sodium. The R_a in this body-centred cubic crystal structure is only 11% of R_a larger than half the interactiomic distance to the 8 nearest neighbour atoms in the $\langle 111\rangle$ type of directions. The R_a is also 2% of R_a larger than half the distance to the 6 next-nearest neighbour atoms in the $\langle 100\rangle$ type of directions. The perpendicular planes through these $8 + 6$ halfway points to the near neighbour then define the atomic polyhedron (or cell) around each Na atom, with volume of course equal to that of the atomic sphere. Also the distance from the centre of an atom into the very corners of the atomic polyhedron is only 14% larger than R_a.

The importance of this discussion of the crystal structure of sodium is that figure 1 shows the

---

*A technical comment is in order here. Electrons are charged particles and hence repel by the electrostatic force. They are also Fermi particles with zero probability of two with the same spin being at the same point at the same time. These two factors mean that what we glibly call 'an electron' is really a quantum 'quasi-particle' with an electron at the centre surrounded by a complex denuded region all moving as a whole (sometimes called its 'dressing' or 'screening cloud'), as emphasised by the Russian physicist L.D. Landau in the 1950s. The subsequent Density Functional Theory of Kohn and others (Kohn and Sham 1965) then gives the one-electron-like Schrödinger-like equation for the Landau quasi-particles in anything from an atom to a crystal. But note that it still has an electron at its centre with a fat 'dressing' so that they still interact when they come close together.

radial wave function to the almost flat, i.e. bonding in form, over the whole range from the distance to the nearest neighbours to the distance into the corners of the atomic cell. We can therefore say firstly that figure 1 is a very good approximation to the actual $\mathbf{k} = 0$ Bloch function over the whole unit cell and hence over the whole crystal. Secondly, we can see that it shows a bonding relationship between the wave function in one atomic cell and that in *all* of its near neighbours. But note the importance in this of metallic sodium having one of the three densely packed crystal structures, i.e. body-centred cubic (bcc), face-centred cubic (fcc) or hexagonal close packed (hcp): the remark about the wave function of figure 1 being a good approximation over the whole crystal would apply equally well in an fcc or hcp structure.[†]

It is important for understanding metallic cohesion that in this wave function each atom is in a bonding relation *simultaneously* to *all* of its 8+6 closely neighbouring atoms clustered around it. Because of a couple of centuries of the development of chemistry in terms of bonds between pairs of atoms, it may be hard to think in metals of an atom being bonded to its surrounding cluster of atoms as a whole, not as a sum of locally separate pair-bonds, but that is what the quantum mechanics is saying.

We can perhaps already infer from this how the malleability of metallic bonding can come about: if an atom is bonded to its cluster of surrounding atoms as a whole, then shuffling the atoms around within that cluster may not cost very much energy as long as it remains hugging closely around the central atom when the shape of a metal specimen is deformed.

So far, so good, but we have only discussed the bonding relationship in one special Bloch molecular orbital, i.e. $\psi_{\mathbf{k}}$ with $\mathbf{k} = 0$. We need to demonstrate that the multi-atom bonding exists through the totality of occupied Bloch orbitals as a whole. In order to keep the rigour of the mathematics as simple as possible while maintaining the quantum mechanical analysis, we will consider first an unusual special metal and later extend the argument to metals generally. We take metallic hydrogen, i.e. hydrogen under extremely high pressure such as may exist at the centre of Jupiter. Figure 2 shows the conceived 'energy density of states' $n(E)$ (very schematic) of Bloch orbitals for metallic hydrogen from completely bonding E_{b} to the maximally anti-bonding E_{ab}. The occupied states with energies $E(\mathbf{k})$ below the Fermi level E_{F} have a net bonding character, while those above E_{F} are empty and net anti-bonding.

If we take our zero of energy as the 'centre of gravity' of this distribution, i.e. roughly the energy of the unbonded electrons, then the cohesive energy U_{b} per electron is something like the 'spread' or 'root mean square' (rms) width $\mathrm{W}_{\mathrm{rms}}$ of the distribution, called 'standard deviation' in statistics, as illustrated in figure 2:

$$U_{\mathrm{b}} \approx -\mathrm{W}_{\mathrm{rms}} \quad \text{per electron.} \tag{1}$$

Note that in talking about bonding in this article we will be focusing on the electrons and thus referring always to the bonding energy *per electron* rather than per atom. We write it as in

---

[†] A small detail: In both 'close packed' crystal structures (fcc and hcp) each atom has 12 equidistant nearest neighbours, whereas in the bcc structure there are 8 nearest neighbours and 6 more close neighbours only 5% further away which taken together act similarly to the 12 equidistant nearest neighbours in fcc and hcp. The atomic radius will be taken to represent the size of all these to a sufficiently good approximation for our purposes, including also the distances to the small intersticies between neighbouring atoms centred on the common corner of several adjacent atomic polyhedra.

equation (1) with a minus sign since the bonded system has a lower energy than a set of free atoms, i.e. we treat ‘cohesive’ and ‘bonding’ purely as descriptive adjectives. Also our argument about the bonding energy being roughly the root-mean-square band width is not only true for a half filled band, but indicates the scale of the energy distribution and therefore applies apart from some numerical factor of order unity to any other fractional degree of band filling such as in an alloy.

We now come to the quantitative crux of the whole matter of metallic bonding. We have seen that the most bonding orbital wave function for sodium (figure 1) has bonding character between any atom and *all its near neighbours*, as is true in the electronic band structure of many materials, and similarly the Bloch function of highest energy in the band in our example of metallic (extremely compressed) hydrogen will be the most anti-bonding possible towards the neighbours. Let us call C the number of such neighbours, i.e. the coordination number $C = 12$ for fcc and hcp metals and effectively something closely like that for bcc. However the energy difference between these most-bonding and most-antibonding Bloch functions will *not* be the correct quantitative measure for the cohesion, because there are vastly more states that are partly bonding and partly antibonding with energies around the middle of the band. For example there are $12!/6!6! = 3991680$ ways of having 6 bonding and 6 antibonding neighbours around a central atom in the fcc and hcp structures! That is why we have the ‘root mean square’ band width in equation (1).

The correct result is that the root mean square width of the energy distribution of Bloch orbitals equals $\sqrt{C}|h|$, where h is the ‘bonding’ or ‘hopping’ integral between the central atom and a neighbour (attractive, and thus usually taken as negative), and with an extra factor of approximately unity assumed for different crystal structures and for any other fractional degree of filling. It gives approximately the cohesive energy U_b per electron for a half-filled band (Heine 1980, pp 82-83, which may have beeen the first time in print explicitly with the square root) and as proved in the mathematical appendix A,

$$U_\mathrm{b} \approx -\sqrt{C}|h| \quad \text{per electron,} \tag{2}$$

where h is the effective hopping energy between neighbouring atoms. This is the central point of the present paper. We will always express the cohesion as an energy *per electron* in the band while we are interested in the nature of the bonding, not any particular material. It is certainly an approximation, but one with an impeccable mathematical pedigree. For the cognoscenti, it derives from successive steps in the Local Moment Method (Cyrot-Lackmann 1968) or/and the Recursion Method (Haydock 1980) for calculating the local density of states at an atom by a sequence of increasingly more accurate improvements, terminated for equation (2) after the second level.

Note that the multi-atom bonding is a *huge* effect. In a traditional picture of forming pair-bonds between atoms, the maximum bonding that can be achieved is $|h|$ from each electron, but the result in equation (2) is $\sqrt{C}$ times as large due to the multi-atom nature of the bonding, where for example equation (2) gives 3.46 times as large for a close-packed metal with $z = 12$! Note also that it is the total number C of neighbours that enters equation (2), not their geometrical disposition (until the higher levels of approximation). Of course multi-atom bonding is not entirely new: see for example Jones (2018, 2022). In Pauling’s (1960) book, the second half of chapter 10 concerns ‘electron deficient structures’, coming immediately before chapter 11 on metals. Aluminium metal, with only three electrons per atom for forming bonds to its twelve nearest neighbours, is well bonded but clearly very ‘electron deficient’.

Where does the factor $\sqrt{C}$ in equation (2) come from, if the relationship between neighbouring atoms in our picture is simply covalent bonding? In a simple hydrogen molecule, as Schmidt, Ivanic and Ruedenberg (2014 a & b) have documented in great detail, the origin of its binding is due to the lowering of kinetic energy coming from where the two electrons are drawn out into the space between the two hydrogen nuclei. For more details see the discussion in the mathematical appendix B, particularly near the end. The wave function is therefore more spread out there than in a free atom, and in quantum mechanics the more spread out something is, the lower its kinetic energy. This is the general principle of covalent bonding, and the $\sqrt{C}$ in equation (2) is due to the bonding being able to spread out even further in a closely packed metal over several close neighbours in what we have called *‘cluster’ bonding.* It is a perfect example of “Covalent bonds are created by the drive of electrons to lower their kinetic energy through expansion”, which is actually the title of the paper by Schmidt et al. (2014a). That effect is automatically included if one calculates the band structure and total energy in a bulk metal in the sense of Kohn and Sham (1965). There is no additional metallic orbital or bond, but there is an additional phenomenon, namely the cooperation between nearby covalent bonds in a metal, as expressed by just the ‘cluster bonding’ effect of the $\sqrt{C}$ in equation (2), and as mentioned, for example, qualitatively by Pauling (1949) for lithium. Its effect also becomes important in situations where the bulk coordination is not present at surfaces or defects (Cyrot-Lackmann 1968), or on the other hand in plastic deformation where the bulk density is maintained. Clearly in small clusters of atoms with various coordination numbers the effects can be more complicated, but one can discern the same trend (see figures 8 and 12 of Jones 1993). This seems fully consistent with the discussion of metal bonding by Allen and Burdett (1995 and correspondence referenced there).

A different aspect of the electronic structure of metallic aluminium is illustrated in figure 3, which shows a very impressionistic snap-shot of how the three electrons per atom might be conceived as being distributed between the 12 neighbours of every atom. The reality is a quantum mechanical mixing (‘chemical resonance’) between all conceivable such distributions, but *all* contained simultaneously within the one ground state of the system. In other contexts it is also called ‘correlation’. What this means precisely is given by the mathematical discussion of equations (26) and (27) in section 4, following that of Pauling 1960 (pp 10-13). The expression ‘chemical resonance’ may seem a somewhat unfortunate one to a physicist, although originated by Heisenberg (1926), because there is nothing in it corresponding to the unique ‘resonant’ frequency response of a tuned electrical circuit or of many elastic structures: but no alternative expression seems to have widely replaced it. Perhaps one could say the system in its one ground state is ‘reverberating’ between all the electron distributions such as that shown in figure 3. Indeed such mixing in the one wavefunction of the unique ground state has been described by Schrödinger (1935) as “the characteristic trait of quantum mechanics”, with nothing corresponding to it in classical mechanics.

All forms of energy in the study of materials ultimately consist of potential and kinetic energy, often mixed in a complicated way as illustrated for covalency at the end of appendix B. But the two forms discussed above are entirely separate physical (or/and chemical) effects, namely the covalency of 'cluster bonding' and the 'correlation' depicted in figure 3. To underline their separateness, we may mention in passing the third and fourth form of energy in solids, namely 'exchange' as leading to ferromagnetism in iron for example and 'superexchange' responsible for antiferromagnetism in some transition metal oxides, but these will not be considered in the present work.

The difference between a metal and a semiconductor or insulator such as diamond can also be seen clearly in the total wave function. In a many-electron system, the total wave function for the system as a whole is expressed (in lowest form) as a single determinant of all the occupied one-electron states below the Fermi level E_{F} as was shown for a metal in figure 2. In the case of diamond the Fermi level falls between the (doubly, for spin) occupied states in its valence band, and the empty states with energy $E_n(\mathbf{k})$ above the substantial energy gap (figure 4). Now a basic property of determinants is that one can take linear combinations of the rows and columns as much as one likes, without affecting the value of the determinant. In the case of our example of diamond, we can transform in this way the determinant of Bloch functions to a determinant of local bonding molecular orbitals between each pair of neighbouring carbon atoms: they are mathematically equal, and a picture of local pair-wise bonds results. However the mathematics depends on having a set of full bands below E_{F}, and hence cannot work for a metal where E_{F} falls within some band(s) and makes electrical conduction possible.

There have been efforts to depict electron localisation in real space and its opposite, the kinetic energy of delocalisation (Savin et al. 1992, Silvi and Gatti 2000). However it is not clear how this can distinguish between kinetic energy reduction in forming a covalent bond as in the hydrogen molecule (Schmidt et al. 2014 a & b), the kinetic energy from orthogonality in the Bloch phase factor $\exp(i\mathbf{k}\cdot\mathbf{r}_l)$ as in a diamond crystal, and the additional 'metallic' effect discussed here.

So far we have talked in largely qualitative terms, but in fact the result (equation (2)) follows from a two-step quantum mechanical proof given in appendix A. Actually it was originally discovered in an entirely different context (see the review Heine 1980, pp 82-83), namely quantum mechanical treatment of solids without the assumption of lattice periodicity such as at the surface of a solid. There is no assumption of lattice periodicity of the structure: at our level of approximation, it is only the number C of bonding neighbours to each atom that matters, which can vary from atom to atom, for example at a surface it is different from that in the bulk. In fact the square root form (equation (2)) is re-expressing the lowest level of approximation of the 'Method of Moments' developed in the 1960s by Cyrot-Lackmann (1968) and others in the group of Prof. J. Friedel using the moments of the electron energy distribution in a systematic way. The Moment Method was developed later into what is now referred to as the 'Recursion Method' (Haydock 1980). See also Bullet (1980) and Kelly (1980) for other reviews of this 'local' approach to the electronic structure of solids, and Finnis (2003). The use of the moments of the electronic structure has increasingly joined the mainstream: see Sutton et al. (1988) and Harrison (1983) for the square root of equation (2).

The form of the result (equation (2)) is rigorous for a distribution of one type of electron only, such as the s-band discussed so far, or indeed for a band of d-electrons only, as shown in appendix A. The latter is quite a good approximation for most of the transition metals where the number of sp-electrons is usually only about 0.5 per atom. In that case the h in equation (2) has to be replaced by a combination of the $(dd\sigma)$, $(dd\pi)$ and $(dd\delta)$ hopping integrals for the five d-orbitals with angular momentum quantum number m from -2 to $+2$ around an axis joining two atoms (Ducastelle and Cyrot-Lackmann 1970 and 1971, and see appendix A):

$$h_{\text{eff}}^2 = [(dd\sigma)^2 + 2(dd\pi)^2 + (dd\delta)^2]. \tag{3}$$

Unfortunately the analogous treatment gets rather more complicated for the mixed sp-bonded metals such as the alkalis and others in groups 2 and 3 of the Periodic Table, as discussed in section 5. However we have a computational study of 17 structures of aluminium also to be discussed there, ranging from the diatomic molecule, through various one-, two- and three-dimensional periodic structures to the actual fcc crystal (Robertson et al. 1993). The results were found to follow surprisingly closely the square root form of equation (2) too! In fact the computed energies (here expressed in eV per atom) are shown in figure 5 with a fit to

$$E(C) = -54.74 + A\sqrt{C} + BC \quad \text{(eV)} \tag{4}$$

$$\text{where} \qquad A = -1.41 \;\text{ and } B = 0.09. \tag{5}$$

Hence all the discussion of the present paper will be based on the simple square-root form of equation (2). The smaller last term in equation (4) is widely interpreted as having quite a different origin, namely the electrostatic repulsion between neutral but somewhat overlapping neighbouring spherical atoms (Jacobsen et al. 1987, Sutton el al. 1988).

Some properties of metals are immediately clear from equation (2). Almost all metals have one of the three densely packed structures fcc, bcc and hcp because these maximise the coordination C. The malleability of metals is equally clear: it is merely shuffling the closely packed neighbours around each atom as the centre of a dense cluster of very nearly C close neighbours without assuming periodicity, i.e. the value of C does not change much. When bending a piece of metal, the total volume and hence average value of C throughout a specimen hardly changes. Nor is it surprising that many metals have phase transitions between the three densely packed structures as a function of temperature or quite modest pressures: they all have $C = 12$ including the bcc structure in the approximate sense discussed above.

We might also note how equation (2) warns what is the wrong way (!) to approach describing metallic structures, namely to add to a conventional pair-bond picture some quadratic three-body or bond-angle terms in the total energy. Figure 6 shows a linear functional form proportional to the number of neighbours, irrespective of the number of electrons per atom, and the quadratic variation for 3-atom or bond bending energy, as well as our square root form equation (2). Note how the correct square-root curve bends upwards with increasing C, which is radically different from the other forms. Also shown in the figure is a 'saturation' model behaviour, i.e. an element with (for example) three electrons per atom could form the usual type of pair-bonds with up to three neighbours which might then 'use up' their conventional pairwise bonding capacity.

A slightly less obvious consequence of the square-root form of equation (2) is the surface reconstruction seen on the [110] surfaces of some fcc metals. If one just sliced through an fcc structure to create a semi-infinite solid with a [110] surface, it would leave atoms at the surface in two types of position, namely with 7 and 11 remaining neighbouring atoms respectively.

Figure 7 shows how such an unreconstructed surface is energetically unfavourable when the energy has the square-root form of equation (2). Instead there is a re-arrangement, for example to a surface structure in which all the surface atoms have an intermediate number $C = 9$ of neighbours.

In sections 2 we will discuss some insight into what held up the computer modelling of defects in metals for a long time from attempts in the 1950s until the work of Daw and Baskes (1983, 1984). The 1950s saw the development of nuclear reactors for use in generating electricity, an important priority at the time. Of course the very energetic fission products cause considerable damage in the structure of the reactor moderator, but attempts at computer modelling were rather unsuccessful. Crucial was the energy of an atomic vacancy. It is easy in a traditional pairwise bonding model to count up the number of bonds lost, which gives a vacancy formation energy equal (but opposite sign) to the cohesive energy of the metal, but in reality it is only about *half* as large or less (Finnis 2003). Daw and Baskes had to introduce a new expression to define the effective amount of bonding that a metal atom makes in a dense metallic structure, and for that Finnis and Sinclair (1984) proposed the use of equation (2). An ab initio analysis by Jacobsen et al. (1987) then justified the approach of Daw and Baskes, but in a wider way than a specific form such as equation (2).

Section 3 will introduce an absurdly over-simplified theoretical model of the dissociation energy of a diatomic metal on the surface of the same metal, where however equation (2) leads to a surprisingly large reduction compared with that for dissociation in the gas phase. Once one understands the origin of that reduction in terms of our equation (2), one can see it as a general effect of metallic cluster bonding. The curvature of the square root form in equation (2) means that the two dissociated fragments retain most of their bonding, i.e. to the metal surface, and lose only a relatively small amount in the dissociation.

We have already noted that the bonding energy (equation (2)) is a quantum lowering of the kinetic energy from the greater spreading of the bonding orbital in a metal over the whole cluster of nearest neighbours. In section 4 we consider that further, and also the role of the potential energy, i.e. the electrostatic repulsion between the electrons. The key point here is that in a metal the electrons can dynamically “keep out of each others way” by hopping into a nearby vacant local orbital as discussed in connection with figure 3. In diamond the electrons are all locked into their localised orbitals within the single determinantal total wave function, whereas in a metal there are plenty of ‘fluctuatingly’ empty orbitals nearby as part of the unique ground state. Keeping (partially) out of each other’s way is called ‘correlation’, including both the effect of the electrostatic repulsion and the specifically quantum effect noted by Schrödinger (1935) in the quotation given above.

We can see the effect in graphite. It is a two-dimensional metal, and because of the lower energy due to correlation, it is the stable form of carbon, with lower energy than diamond for all the latter’s infinite spread of perfect tetrahedral C-C bonds. Furthermore the benzene molecule is a miniature 6-membered ring of metal, with a half-filled band of π-orbitals. The ortho-, meta-, para reactivity oscillation around the ring from an attached side group is mathematically and physically analogous to the Friedel (static) oscillations of electron density around an impurity in a metal (Friedel 1954). Benzene’s stability can be understood in terms of Pauling’s concept of chemical 'resonance' (Pauling 1960), but in the case of benzene he seems to have missed the main point. Perhaps the classical word 'resonance' trapped him here into a classical way of thinking rather than seeing and feeling the world as a quantum particle does (section 4).

In section 5 we turn to the metals such as aluminium with a mix of s and p electrons as found in the alkali metals and others in groups 2 and 3 in the Periodic Table. The simple analysis of appendix A leading to the square root form in equation (3) simply does not apply, as already remarked below equation (2). Robertson et al. (1993) in Cambridge therefore carried out the 'computer experiment' to discover the actual situation, with results already shown in figure 5. However in section 5 we discuss how the mathematics of appendix A becomes much more complicated when stretched to apply to a mixed band of s and p electrons, but some conclusions can be drawn. We also report the work of Jacobsen et al. (1987) with their approach from Density Functional Theory, leading to a justification of the approach of Daw and Basques (1983, 1984) mentioned in connection with section 2, but without reaching specifically the square root approximation (equation 2).

In section 6 we bring together the various strands into a cohesive picture, with some historical perspective about the surprisingly drawn out development of the present story from Bloch (1929) to an insight about the *sp*-bonded metals when the present manuscript was nearly complete. We have already noted in connection with figure 1 that the single $\mathbf{k} = 0$ Bloch function shown there around an atom of metallic sodium, calculated by Wigner and Seitz in 1933, already displays simultaneous bonding to *all* its surrounding close neighbours, which we have called 'cluster bonding'. It is inherent in the mathematics of Bloch's theorem plus symmetry (group) theory (Heine 1961).

2 Modelling cohesion in metals

In this section we pick up the story from section 1 of the problem of the computer modelling of defects in metals. We will focus first on the formation energy $U(\text{vacancy})$ of a vacancy (missing atom), originally a puzzle but also a source of insights which ultimately led to modelling generally the total cohesive energy of a metallic structure. Besides the interest in the radiation damage caused inside a nuclear reactor, the development of electron microscopy in the 1950s made possible the wider study of dislocations and other defects formed in the deformation of metals.

A pivotal fact about vacancies is that the experimentally measured energy of a vacancy in a metal is very roughly only about one-third of the observed cohesive energy U_c of the metal,

$$U(\text{vacancy}) \approx \frac{1}{3} U_\mathrm{c} \qquad\qquad \text{(experimental)} \tag{6}$$

for quite a wide range of metals according to Finnis (2003, below equation (5.81)). This observation was rather puzzling on simple theoretical grounds because one might expect to find

$$U(\text{vacancy}) \approx U_\mathrm{c} \qquad\qquad \text{(traditional)} \tag{7}$$

from counting up the number of bonds lost per atom if one just pictured the two processes of plucking out one atom to create a vacancy on the one hand (figure 8), and pulling the whole solid apart on the other hand. We shall call this the ‘traditional’ approach, with every atom assumed (correctly) bonded equally in some way to each of its 12 neighbours because this is consistent with the cubic symmetry of the material, and incidentally also with our quantum discussion in section 1 of the $\mathbf{k} = 0$ electron Bloch function (figure 1) calculated by Wigner and Seitz (1933) for sodium. For the bulk cohesive energy in equation (7) we destroy $C = 12$ bonds of every atom to its neighbours, but a bond has two ends and we must not count it twice. Thus we obtain

$$U_{\mathrm{c}}(\text{theory}) = 6U_{\mathrm{b}} \quad \text{per atom,} \qquad \text{(traditional)} \tag{8}$$

where U_{b} is the energy of one bond (counted positive as energy contained in the bond). On the other hand plucking an atom out of the bulk destroys 12 bonds at the vacancy, but we are not in the business of destroying atoms and hence we get back half of that energy when adding the removed atom to make one additional bulk atom for the specimen. We therefore have for the vacancy a net creation energy cost of

$$U(\text{vacancy}) = 6U_{\mathrm{b}}, \qquad \text{(traditional)} \tag{9}$$

and hence from equation (8) for the result of a traditional analysis:

$$U(\text{vacancy}) = U_{\mathrm{c}}. \qquad \text{(traditional)} \tag{10}$$

This was essentially the theoretical understanding of the formation energy of a vacancy in the 1950’s and really up until the work of Daw and Baskes (1983), but unfortunately the ‘traditional’ result (equation (10)) is wrong by more than a factor of two compared with the laboratory measurements (equation (6)) for a range of metals.

The important step is that we now repeat the two calculations (for the cohesive energy and the vacancy formation energy) by applying the quantum approach of equation (2) with the cohesion proportional to the *square root* of its coordination number applied to every atom. It is a bit easier to follow the arithmetic if we express it in terms of C, and then put $C = 12$ at the end. First the cohesive energy: each atom in the bulk has C nearest neighbours and hence the cohesive energy is (per atom)

$$U_{\mathrm{c}} = \sqrt{C}|h|, \qquad \text{(quantum)} \tag{11}$$

using the notation of equation (2). Turning to the vacancy, we would say that the atom plucked out to form the vacancy has lost all of its C neighbouring atoms, but it effectively gets back the same number when added to the specimen elsewhere as an additional bulk atom. However we also have (figure 8) that the C atoms surrounding the vacancy are left with only $(C - 1)$ near neighbours each instead of C in the intact bulk, and hence the formation energy of the vacancy is

$$U(\text{vacancy}) = C[\sqrt{C} - \sqrt{C-1}]|h|. \qquad \text{(quantum)} \tag{12}$$

Since $C \gg 1$, we can write

$$\begin{aligned}\sqrt{C-1} \quad &= \sqrt{C}(1-\tfrac{1}{C})^{\frac{1}{2}} \\ &= \sqrt{C}(1-\tfrac{1}{2C}+\ldots)\end{aligned} \tag{13}$$

from the binomial expansion of the square root factor in the middle of equation (13). Substituting the result into equation (12) gives the vacancy energy to a good approximation as

$$U(\text{vacancy}) \approx \frac{1}{2}\sqrt{C}|h|, \qquad \text{(quantum)} \tag{14}$$

and hence finally from (11)

$$U(\text{vacancy}) \approx \frac{1}{2}U_{\text{c}} \qquad \text{(quantum)} \tag{15}$$

which is in much better accord with the observations (equation 6). We must not expect any greater accuracy because the square root in equation (2) is only the lowest level of approximation from the 'Method of Moments' or 'Recursion Method' of formulating the quantum mechanics when applied to the situation. See references in section 1.

What have we learnt from this fairly long story about the vacancy formation energy? Clearly, we do need quantum mechanics to get even qualitatively near the right answer! Specifically the total coordination number of near neighbours appears to play the principal role, both in the theory of equation (2), and in the observed fact that the differences between the actual fcc, hcp and bcc structures do not seem to make a big difference in the observed vacancy formation energy (equation 6) (Finnis 2003), a point which we might also have expected from the easy phase transitions between the three structures for several metallic elements. Of course the total coordination number C cannot be the complete answer: as remarked above and in section 1, equation (2) is only the first level of approximation in the local description of the electronic structure (see references given there).

The breakthrough in formulating a scheme for modelling deformed metallic structures came with Daw and Baskes (1983, 1984) proposing the form

$$U = \sum_i G_{\text{eff}}(C_i) + \frac{1}{2}\sum_i\sum_j \Phi(R_{ij}) \tag{16}$$

with

$$C_i = \sum_j w(R_{ij}). \tag{17}$$

Here the 'glue' function G depends on an effective total number of neighbours (equation (17)) to each atom without their geometric distribution. For this it just counts up the neighbours j around atom i with weight w depending on their distance R_{ij}, and with w normalised to unity such that

$$w(r) = 1 \tag{18}$$

at the normal interatomic spacing of the bulk metal. Finnis and Sinclair (1984) then rapidly proposed using the square root form equation (2) for the 'glue' function G in equation (16) or something like it. The $\Phi(R_{ij})$ is imagined as a pairwise short-ranged repulsion between neighbouring atoms as remarked below equation (4). Note that G depends on the *total* number C_i of neighbours to atom i with no specific bonding to specific neighbours. It therefore implies the cluster bonding to the neighbours as a whole as described in section 1. Mathematically the Φ in equation (16) can be absorbed into C_i as an additional term in equation (17), but in view of the different kinds of interaction w and Φ are supposed to represent (bonding and short ranged repulsion) it seems convenient to model them separately in practical use. The whole formulation has appeared rather successful (Daw 1989, Foiles 1989), and can now be derived from a simplified 'local' theory of the electron system of Thomas-Fermi type (Finnis 2003, p.257).

Two questions remain. Firstly it was emphasised in section 1 that the mathematical derivation of our basic equation (2) for metallic bonding applies only to systems having electrons of only one type, to which the transition elements with mostly d-electrons approximate fairly well. But what about the *sp*-bonded metals such as aluminium and zinc with mixed s and p electrons? We shall take that up in section 5, having already 'stolen the show' in section 1 with the range of 'computer experiments' on aluminium in figure 5 which when fitted to equation (16) gave a glue function (equation (4)), equation (5) remarkably similar to the square root. But that to date relates only to aluminium.

The second issue is to clarify the theoretical justification of equations (16) and (17) from basic quantum mechanics, i.e. from the ab initio density functional theory of Hohenberg and Kohn (1964). The most complete discussion is probably that of Jacobsen et al. (1987) and section 8.2 of the book Finnis (2003), which show that one can indeed derive the general form of equations (16) and (17), in particular with the Thomas-Fermi approximation for the electron gas. But one must not ask for the logically impossible. We have emphasised for example that the square root form in equation (2) is just the lowest level of approximation for solving for the electronic structure of some material, atom by atom, and in that sense it can be a remarkably good one for metals, as shown by the very modest degree of scatter about the curve in figure 5. However beyond that there can only be a general *procedure* for carrying the calculation further, not some general *formula* including all the structural and electronic effects covering all conceivable samples of all possible materials.

3 An insight into catalysis on a metal surface

A molecule (or two) adsorbed on a metal surface can often divide (or re-arrange) in ways that tend to be prevented or inhibited in the gaseous free state by a large energy barrier. How does the proximity of the metal reduce such barrier when the molecule is adsorbed on a metal surface? We will introduce in figure 9 an absurdly over-simplified model of a catalysed reaction on a surface, but one can see explicitly with simple arithmetic how the energetics of metallic bonding brings about the initial dissociation, based on the square root approximation of equation (2).

Mathematically, we have

$$U = |h| \sum_i \sqrt{C_i} \quad \text{per electron-per-atom} \tag{19}$$

summed over all atoms i, as we had when calculating the vacancy formation energy in section

2. Note again that this is not counting bonds from each atom: it is counting the amount of bonding contributed by each electron of that atom. As a preliminary step we start in line (a) of figure 9 with the free molecule in the gas phase, on the left intact as a dimer molecule and on the right dissociated. Thus for the free molecule in the gas phase we have from equation (2) and figure 9(a) the dissociation energy ('left' minus 'right' in the figure)

$$\text{case(a)} \qquad U(\text{diss.}) = 2|h| \quad \text{per electron-per-atom.} \tag{20}$$

Turning now to figure 9(b) we have the dimer adsorbed on the metal surface with the ad-atoms directly above the substrate atoms. To total up (19) for all the atoms we note that the number of 5's and 6's in the top row of substrate atoms is the same when the ad-atoms are combined as a dimer and when dissociated on the right of figure 9(b), so that their contribution to the total (19) is the same and hence cancels out when we take the difference between left and right to obtain the dissociation energy. We also must consider the two ad-atoms with $C = 2$ on the left when combined, and with $C = 1$ dissociated on the right, giving (per electron-per-atom)

$$\text{case(b)} \qquad U(\text{diss.}) = 2|h|(\sqrt{2} - \sqrt{1}) \approx 0.83|h| \quad \text{per electron-per-atom} \tag{21}$$

using $\sqrt{2} \approx 1.414$.

We note this dissociation energy (equation (21)) is substantially reduced from equation (20) by more than a factor of two. The reason for the reduction from equation (20) to (21) is clear from the shape of the square root function shown quantitatively in figure 10: the energy cost of losing one neighbour out of several drops dramatically with increasing C. For example we have (in units of $|h|$)

$$\begin{gathered} \sqrt{1} - \sqrt{0} = 1, \quad \sqrt{2} - \sqrt{1} \approx 0.41, \quad \ldots, \\ \sqrt{6} - \sqrt{5} \approx 0.21, \quad \ldots, \quad \sqrt{12} - \sqrt{11} \approx 0.15, \end{gathered} \tag{22}$$

giving the large energy reduction from figure 9(a) to figure 9(b).

Having the ad-atoms perched directly above the substrate atoms (figure 9(b)) may seem rather unlikely, and hence in the bottom row (c) of figure 9 we have supposed them to sit above the centres of surface atomic squares (adjacent on the left and separated on the right), at a height of $\frac{1}{2}a\sqrt{2}$ such that their distances from the substrate atoms in the top layer and hence the value of h is unchanged. But note that the two ad-atoms now bond to two rows of substrate atoms. Thus we have $C = 4$ for the two ad-atoms in the dissociated state (right side of figure 9) but $C = 5$ as a dimer on the left. Also the coordination numbers of the top layer of substrate atoms now do not cancel out between left and right. We have two 6's on the right replacing a 7 and a 5 on the left, and have two rows like that because ad-atoms make contact with two rows of substrate atoms. Counting only the relevant ten atoms left and right, we find (per electron-per-atom)

$$\begin{aligned} \text{case(c)} \qquad U_{\text{bond}}(\text{dimer: left}) &= |h|(2\sqrt{5} + 2(\sqrt{7} + 2\sqrt{6} + \sqrt{5}), \\ U_{\text{bond}}(\text{separated: right}) &= |h|(2\sqrt{4} + 2(4\sqrt{6}), \\ U_{\text{bond}}(\text{diss.}) &= |h|(-2\sqrt{4} + 4\sqrt{5} - 4\sqrt{6} + 2\sqrt{7}) \approx 0.44|h|. \end{aligned} \tag{23}$$

This is a further major reduction in the dissociation energy from our first result (equation (21)), in comparison with the dissociation (equation (20)) of the free molecule in the gas phase of $2|h|$ (times the electron per atom ratio e/a as before).

It is now clear from following our procedure that the dissociation energy will be even lower on a surface step, and at some sites on a surface of crystallographic even higher order. Sounds familiar? Surface reactions are known to be enhanced at special sites, and also at some extra impurity catalyst atoms placed there.

Dissociation can even give out energy as we shall see. Let us imagine a step on a higher order surface, with our dimer having a more intimate contact with the substrate from lying in that step. If we now count up the number of neighbours at every atomic site as in figure 9, then the two ad-atoms of our dimer will certainly lose one bonding each from a dissociation, i.e. a reduction from some C_s to $C_\mathrm{s} - 1$ where C_s is the number of surface atoms that each half of the dimer is in contact with. It is clear from figure 10 and equation (22) that the energy cost will be smaller the larger C_s is, i.e. the more snugly the adsorbed molecule fits into the step. So far, so good, but we can furthermore imagine two kinks of opposite sign forming a local displacement of the step sideways, say four atomic sites long, with our molecule lying initially at the centre of that little section of step displacement. The dissociation of the dimer will then result in its two atoms bumping into the substrate atoms at the ends of that section, thus each gaining a new contact there (!) with a net effect of one bonding contact actually gained from the dissociation! Of course as in figure 9 and equations (20), (21) and (23), there will also be complicated changes of bonding counts among the substrate atoms. However these would only be balanced changes of ± 1 up or down, giving zero net change in the total number of bonds within the substrate, and hence their total contribution will be rather small.

In conclusion, our grossly simplified model of a metal of *s*-electrons only, i.e. with a single interatomic 'hopping' integral h, has displayed two effects when dissociating while adsorbed on a metal surface. Firstly cluster bonding as expressed in equation (2) means that the breaking of the connection of one atom to a neighbour does not cost a lot of energy, as long as there remain intact bonds to enough other neighbours in the substrate. Secondly to ensure there are enough neighbours like that, special sites play an important role, and can actually increase the number of bonding contacts in a dissociation.

But why does that grossly simplified model have anything valid to say about real metallic catalysts? We have already mentioned that equation (2) remains mathematically valid for a band of five *d*-electrons, and the extensive study of aluminium shown in figure 5 and equations (4) and (5) as (hopefully!) typical of *sp*-bonded metals has shown a behaviour very like the square root form as we shall discuss again in section 5. Indeed we shall refer there to some theoretical analysis which suggests one might expect that.

4 Metallic-like behaviour in graphite and benzene

The structure of one atomic layer of graphite is a hexagonal net as shown in figure 11, and it is a two-dimensional metal, bonded in-plane by a perfect mesh of hybridised $2s$, $2p_x$ and $2p_y$ complete covalent valence bonds. The remaining $2p_z$ orbitals with one electron per atom make up the 'conduction' band. Of course graphite is not a good conductor of electricity, but good conduction is a matter of a long mean-free-path between scatterings around a region of free Fermi surface, which in graphite is broken up and dramatically reduced by Brillouin zone boundaries. However that is not important when, as here, we are concerned with bonding issues at the atomic length scale.

In diamond on the other hand, four electrons per atom in $2s$, $2p_x$, $2p_y$ and $2p_z$ atomic orbitals combine to give four directed valence bond orbitals in the [111], $[1\bar{1}\bar{1}]$, $[\bar{1}1\bar{1}]$, $[\bar{1}\bar{1}1]$ directions. These bond with similar ones from four neighbouring atoms to make diamond the hardest material known. This seemed to one of us (V.H.) as a student the ultimate perfect covalent bonding, with a large energy gap between the occupied valence band and empty conduction band. It was therefore a surprise to learn ten years later that it is graphite which is the stablest form of carbon (at room temperature and pressure), not diamond![‡] This is of course consistent with the general picture of metals being strongly bonded, as painted in section 1.

We turn next to figure 12 which shows the benzene molecule based on one hexagonal ring from the graphite structure. It behaves as a little 'metallic' ring which is the clue to its important resulting properties. The six carbon and six hydrogen atoms all lie in the xy-plane, as do the σ-bonds between them formed from the hydrogen $1s$ and carbon $2s$, $2p_x$ and $2p_y$ atomic orbitals, all these bonds being shown as lines in figure 12. In addition there are the $2p_z$ π atomic orbitals of the six carbon atoms, pointing perpendicular to the xy plane of atoms. These can form six π-bonding orbitals between neighbouring carbon atoms around the ring, not shown in the figure: but note that with only one $2p_z$ electron per carbon atom, there are only enough electrons (3 each of up and down spin) to occupy half of this band of π-orbitals.

A solid state physicist would immediately apply Bloch's theorem to form and describe these (occupied and unoccupied) molecular π-orbitals around the ring with phase factors (Bloch 1929, Ashcroft and Mermin 1965):

$$\exp(ik_n) \quad \text{with} \quad k_n = \frac{2\pi n}{6} \tag{24}$$

and

$$n = 0 \text{ to } 5 \text{ (or } -2 \text{ to } +3) \tag{25}$$

from one carbon π-bond to the next. The energies $E(k_n)$ are as shown in figure 13, together with the 'Fermi level' E_F between the lower doubly occupied (for spin) π-orbitals and upper unoccupied ones.

A complementary, perhaps more chemical, approach is rather different. We start again with the hexagonal framework of hydrogen $1s$ and carbon $2s$, $2p_x$ and $2p_y$ σ-orbitals in the xy-plane, and then think again of the $2p_z$ orbitals from the carbon atoms forming $2p_z$ π-bonding orbitals between some neighbouring pairs. We therefore have three up-spin electrons occupying three such π-bonding orbitals, and similarly three down-spin ones, some example configurations being

---

[‡] Historical note: V.H. learnt this when meeting one of the scientists at the General Electric Research Labs in USA who had achieved the industrial production of diamond grit for manufacturing cutting and smoothing tools for hard steel and concrete etc., and incidentally very nice inexpensive nail files. It had started as a war-time project during World War II, but took ten years to succeed, because one is fighting against the adverse energy difference!

shown in figure 14. Some such configurations would have higher energy than others, for example one with all the six π-electrons on one side of the molecule due to electrostatic repulsion between them, but even here one must remember that 'electrons' are really 'quasiparticles' in the sense of section 1 with their 'dressing' screening their charge to a considerable extent by other nearby electrons, especially those with parallel spin.

The important point is that there are very many different configurations such as shown in figure 14: in fact 400 to be precise! Figure 14(a) shows the historical Kekulé structure, while a configuration with probably even lower energy could have one electron between each neighbouring pair of carbon atoms with spins alternating around the ring (figure 14d). The number 400 arises from the ${}^{6}C_{3} = 20$ ways of distributing the up-spin electrons among the six π-bonding positions between neighbouring carbon atoms, combined with the same number for the down spins, giving $20 \times 20 = 400$. This diversity gives very strong 'chemical resonance' (Pauling 1960, chapter 1), as also shown characteristic of metals in figure 3. It arises when relatively few electrons per atom are strewn across a larger number of possible bonding positions between neighbours, as discussed in section 1.

The strong lowering of energy in 'chemical resonance' results from the variational principle of quantum mechanics combined with a theorem in matrix algebra, as pointed out by Pauling (1960, p 12) which we repeat here almost verbatim. It arises when we write the full wave function Ψ for some system as a sum over several trial or incomplete or approximate but chemically sensible many-electron wave functions ψ_r with r up to some ψ_M, where all of them are contained together in the ground state (equation (26)), the specifically quantum mechanical effect referred to in section 1:

$$\Psi = a_1\psi_1 + a_2\psi_2 + a_3\psi_3 + \ldots a_M\psi_M. \tag{26}$$

In the spirit of the variational principle we can get the best wave function within that form by varying the coefficients a_r to minimise the total energy E_0. Indeed there is a theorem in matrix algebra (Matthews and Walker 1965, p 315) that guarantees adding an extra term to equation (26) can only lower the energy further, i.e.

$$E_0(M+1) \leq E_0(M). \tag{27}$$

In the present instance of benzene it would seem natural to use for the ψ_r in equation (26) the 400 wave functions discussed above in relation to the types of bonding shown in figure 14. It does seem strange that Pauling (1960, p 12) discusses a series like equation (27), but in writing about benzene (Pauling 1960, p 188) confines himself to the two Kekulé electronic structures only, neglecting all the rest of the 400 ψ_r mentioned above, even that of figure 14d with charges and spins that look better spread out. It is interesting in this connection to consider the full molecular orbital type of wave function, a 6×6 determinant in terms of the six filled Bloch-type one-electron molecular orbitals specified in figure 13. It would give a total energy which would be a terrible sum over matrix elements of the Hamiltonian between all possible pairs out of the 400 functions mentioned! Its energy would not be as good (i.e. as low) as with the coefficients adjusted individually as in the manner of equations (26) and (27) to minimise the total energy, but better than that from just one of them, even the Kekulé one of figure 14a, or even that of figure 14d which looks very good from a bonding point of view, but missing the ‘chemical resonance’ analogous to figure 3.

We turn to the kind of metallic properties shown by benzene and its compounds due to the high degree of adjustability in the chemical resonance in its π-band of $2p_z$ orbitals. Firstly it means the benzene molecule is very adaptable about replacing one or more of the hydrogen atoms by other side-chains such as in toluene (figure 13), or even replacing one or two of the carbon atoms by nitrogen or indeed other element even further afield in the Periodic Table. Its π-band has a degree of electron fluidity, just as in metals the screening by mobility of the conduction electrons results in adapting to a wide range of differing atomic species and hence in a wide range of alloys.

A second property of benzene is directly analogous to the so-called Friedel oscillations in metals (Ziman 1964, p 137). A substitutional impurity as a guest atom in a metal causes a (static) ‘splash’ in the electron density of the host around it, with an electron density undulation with wave-vector $2k_\mathrm{F}$ where $2k_\mathrm{F}$ is the diameter of the Fermi surface. Similarly the replacement of one of the hydrogen atoms of benzene by a side-group which tends to attract or push out some electron density, results in an oscillating chemical reactivity at 1, 2 or 3 steps further around the ring, the so-called ortho, meta and para positions.

Of course the benzene molecule is not malleable(!) but from the point of view of the electrons in the partially filled π-band the situation is not so different. Their mobility serves to adapt them, or to bond partially, to any side-group which is replacing the hydrogen atom in a sigma bond to one of the carbon atoms of the basic xy-framework, or more than one such side-group. It is akin to the ‘screening’ of an impurity or other local change in a metal as mentioned above.

Another ‘metallic-like’ effect arises from the saturation type of curvature of the square root curve as mentioned in section 3 in connection with figure 10, i.e. the small energy cost when reducing from a larger coordination such as C to $C-1$. If one throws a log of wood on a fire it becomes red hot as the organic matter burns to carbon dioxide and water vapour, and when one digests one’s meal most of it ultimately also gets exhaled as carbon dioxide and water vapour. But in the latter case, the energy is released in a thousand small steps to fuel the myriad of metabolic processes in all the cells of one’s body. These involve substantial chemical changes but mediated by the ‘fluid’ nature of the π-band of many benzene-type rings found throughout biochemistry.

5 The *sp*-bonded (‘Nearly Free Electron’) metals

This section covers a point left hanging at the end of section 1, specifically how far the ideas about metallic bonding developed in section 1 from the square root in equation (2) can be applied to the *sp*-bonded elements such as zinc or aluminium. The issue was that our basic equation (2) was derived in appendix A from the quantum mechanics of a material with only one type of valence electron, though this is quite a good approximation for the transition metals. However that restriction is manifestly false for the ‘Nearly Free Electron’ (NFE) metals with their conduction electrons predominantly of mixed s and p atomic character such as Zn ($4s$ and $4p$) or Al ($3s$ and $3p$). The coordination number C and particularly its square root $\sqrt{C}$ have been the basis from equation (2) for our understanding the working of metallic bonding in several ways.

Thus sections 1 to 4 include diverse applications to crystal structures, surfaces, vacancy energy, phase transitions, the 'glue' model of Daw and Baskes (1983, 1984) for computer modelling of deformation in metals at the atomic level (section 2), and the bonding changes underlying catalysis on metal surfaces (section 3), plus some aspects of the chemistry of benzene (a little 6-membered ring of metal) which remind a physicist of some metallic properties.

To what extent can we regard these explanations based on equation (2) as also valid applied to NFE metals? Here we must accept the results of the ab initio computer experiment on 17 structures of aluminium shown in figure 5 and equation (4) as hard facts, at least for this metal, nearly as 'hard' as the basic quantum mechanics in appendix A but here in its modern computational form of Kohn and Sham (1965) as remarked in section 1.

We note that the results (figure 5 and equations (4) and (5)) fit the square root form equation (2) unexpectedly well, at least for this particular metal. They cover 17 structures of aluminium (plus the free atom), ranging from the di-atomic molecule through a line of atoms, a 'ladder' structure, and other one- two- and three-dimensional periodic structures all the way to the fcc crystal with $C = 12$ neighbours, all calculated at the same interatomic distance for comparability (Robertson et al. 1983). For example a graphite-like layer was chosen for $C = 3$, and a square lattice for $C = 4$, a double-layer of it then giving $C = 5$. Three structures all have $C = 6$, namely a closely-packed layer, the simple cubic structure, and a [110] double-layer from the fcc structure. A double-layer of close packing gave $C = 7$, while four structures had $C = 8$: a [100] double-layer from the fcc structure, a lattice of vacancies in the fcc structure, a simple-hexagonal structure, and the bcc structure. The final structure with $C = 12$ was fcc. Although most of these are rather obscure geometries as such, they do cover the local situations occurring for an adsorbed atom on a surface, or atoms in the surface, or atoms around a crack or other defect.

Secondly we note that there appears rather little spread about the curve in figure 5. This demonstrates (i) that it is the total number C of near neighbours that really is the dominating factor rather than any directional arrangement. (ii) It justifies the assumption by Daw and Baskes (1983, 1984) that it is the total number of near neighbours which should enter their scheme of computer simulation of plastic deformation in metals, as in equations (16) and (17) in section 2. (iii) It means that in the Local Moments Method of calculating the local density of states at an atom (section 1) the contributions of higher moments appears to be rather small. (iv) It supports the theory of Jacobsen et al. (1987) of the electronic structure of metals (see below).

Thirdly we note that the fit (equations (4) and (5)) to the computed results contains a smaller, spherically symmetric, repulsive energy which is expected as coming from electrostatic repulsion between the electron clouds of the atoms (Jacobsen et al. 1987, Sutton et al. 1988).

Fourthly there is an interesting feature of figure 5 in that the first four points ($C = 0$ to 3) fit nicely on a straight line, with a nice interpretation. Aluminium atoms with three electrons can form up to three conventional (2-atoms, 2-electrons) covalent pair bonds with an energy (from the figure) of 0.67 eV per electron-per-atom each.

A wide-ranging theory covering all the above, and more, was developed by Jacobsen et al. (1987), starting from Density Functional Theory (Finnis 2003). In the first half of their paper, with a succession of transformations guided by the Variational Principle, they developed a mathematical model applicable to *both* transition metals and to the *sp*-bonded metals of interest in the present section. They emphasise that their theory therefore derives the model (equations (16) and (17)) originally proposed empirically by Daw and Baskes (1983, 1984), with the bonding energy expressed as a function of the total number of near neighbours, suitably defined, i.e. "cluster" bonding. The overlap of the electron clouds of neighbouring atoms also yields the short-range repulsion of electrostatic origin mentioned above.

However the square root law (equation (2)) does not appear explicitly in their paper (Jacobsen et al. 1987). They are concerned to set up a theory useful for all sorts of calculations on different aspects and properties of specific metals, not a 'broad brush' discussion of metallic bonding. As a particular example they calculated the atomic relaxation occurring at a [110] surface of aluminium. They found satisfactory agreement of their calculations with the measured relaxations, from which we may conclude that the effects we have explained in figure 7 with the square root in our equation (2) are also inherent in their theory. In fact at present we do not know how well the square root law holds for other NFE metals.

The results of the ab initio computer experiment on aluminium follow a square root form so well in figure 5 and equations (4) and (5) that it seems more than a coincidence, which suggested having another look at the theory of appendix A. In fact it turns out that the theory of appendix A can be modified and extended to cover a NFE metal such as aluminium with a conduction band that is a mixture of $3s$ and $3p$ states (or to include both the s and d states of a transition metal). However the algebra becomes more complicated and wordy, plus having an additional approximation. In any case we already know from figure 5 what the result is for aluminium, and hence we will not go through the analysis word by word, but content ourselves with the following outline remarks.

The suffix i in the Hamiltonian matrix element H_{ij} now really stands for i equal a particular atomic state, i.e. the atom's position x, y, z in the crystal structure *and* the n and l quantum numbers of the particular s or p or d state, *and* its m quantum number of the particular state.

The same set of numbers then stand for j if we have a diagonal matrix element of H: or the similar set of position and quantum numbers for j if H_{ij} is an off-diagonal matrix element of H.

The value of the H_{ij} matrix element also has a different form depending on whether or not it is a diagonal type of matrix element H_{ii}, i.e. whether on the same atom and with all the same quantum numbers enumerated above, or whether non-diagonal. The non-diagonal matrix elements between different atoms contain 'hopping' matrix elements such as $ss\sigma$ or $dd\sigma$, $dd\pi$ or $dd\delta$ between the two atoms, each then squared when we form $H_{ij}H^*_{ji}$ summed over all the atomic quantum numbers listed above. Summing over j then gives a sum of *squared* terms such as in equation (3). The important point about them is that each occurs C times, once from each of the C neighbours of atom i, as in appendix A.

The fully diagonal matrix elements in H_{ii} (i.e. diagonal in all the quantum numbers listed above) have a completely different role and different form. The objective is to calculate the 'spread' or 'breadth' of the distribution of one-electron energy levels of the system at atom i, in order to get an approximate value for its bonding in the sense of figure 2. For this we need the spread about the mean energy, i.e. relative to the mean energy as zero. To achieve that we need to subtract something from the fully diagonal parts of the H_{ij} described above, i.e. some average value of the relevant atomic energy levels E_s and E_p or E_d. The upshot of that adjustment is that our final result for the bonding energy has the form

$$E_b \approx -a - \sqrt{b + cC}. \tag{28}$$

The main point about this result is that C is of order maybe 10 to 12, and hence the last term in equation (28) dominates the other ones which are basically of 'one-atom one-electron' nature. We therefore have again all the consequences of the square root shape discussed throughout the paper.

Actually it is even a bit better than that. Consider the function

$$y = -a - \sqrt{b + cx} \tag{29}$$

like equation (28), which can be written as

$$y + a = -\sqrt{c(x + \frac{b}{c}))}, \tag{30}$$

but note that it is exactly the same as the function

$$y = -\sqrt{cx}, \tag{31}$$

but moved up an amount a and to the left an amount b/c! Thus *all* the arguments made in section 1 and subsequently from the cohesive energy having the simple form of equation (2) remain valid.

Incidently, we have remarked elsewhere that the 'spread' we are calculating is the 'standard deviation about the mean' in statistics, which is the square root of the 'variance', which is the second moment of the distribution. In the Method of Moments for calculating the local electronic structure of a solid, the n'th moment can be visualised as evaluating a path from a state on one atom and returning to the same state after n steps following non-zero matrix elements of the Hamiltonian (Cyrot-Lackman 1968). Such a picture may be of help in understanding the calculation.

6 Conclusions and historical perspective

The first of three concepts emphasised in section 1 onwards (to be referred to as (a), (b) and (c)) is that of 'cluster bonding'. The driving force is the same as in other covalent bonding from the hydrogen molecular ion H_2^+ onwards, originating in the electron kinetic energy driving the spreading and the smoothing of the wave function between the two hydrogen nuclei (Schmidt et al. 2014 a & b, and our appendix B). Particular examples going beyond the usual '2-centre 2-electron' situation have been discussed sometimes as 'hypervalent' when binding more than two atoms or two electrons (Jones 2022).

But metals exhibit the concept of 'cluster bonding' in its simplest and most extreme form which we can characterise as simply 'the more, the merrier' in the number of neighbours. Its multiplicative factor $\sqrt{C}$ in equation (2) is a huge effect, as noted in the next paragraph below that equation. We noted that it automatically implies metals having one of the three 'close packed' crystal structures fcc, hcp, bcc (section 1) with several phase transitions between them in some elements at moderate temperatures and pressures. It also automatically explains the malleability of metals, when the cluster of neighbours around each atom gets distorted but rarely broken up. Moreover its manifestations apply across the three transition metal series bonded predominantly by *d*-electrons as well as to most of the *sp*-bonded metals down columns I, II and III of the Periodic Table including both the A and B sections. It is a broad but well specified phenomenon, with the counting of the *total* number of near neighbours becoming the cornerstone of Daw and Baskes' (1983, 1984) approach to computer modelling of metallic structures in plastic deformation.

The second broad theme (b) of the present paper has been the upward curvature in the square-root shape $-\sqrt{C}$ of the approximate form (equation (2)) of the bonding energy in its dependence on the coordination number C of near neighbours as shown in figures 6 and 7. Among various consequences it means for example that atoms at the surface tend to coalesce into a layer as dense as possible as in figure 7. In the bulk it results in metals having predominantly the three close-packed structures as mentioned above. The situation is quite unlike the diamond structure for instance, mentioned in section 1.

Another effect, becoming our third theme (c), also results from the upward curvature of the bonding curve $-\sqrt{C}$ in that the curve becomes flatter towards the end $C = 12$ of its range. This was the crux of our interpretation of surface catalysis in section 3, especially at a kink site on a surface step. Here any adsorbed atom or molecule would have a substantial contact number C with atoms of the substrate. The nature and number of new contacts would be largely retained in a dissociation (or chemical re-arrangement) on the surface, which therefore costs relatively little energy in the reduction from $-\sqrt{C+1}$ to $-\sqrt{C}$ as shown in figure 10 of section 3.

Of course it is very important that the above three broad principles have a sound quantum mechanical theoretical basis. This is provided in the mathematical appendix A for any metal having only one type of electron, to which the transition metals approximate quite well. The square root form $-\sqrt{C}$ in the cohesive energy can also be seen to come from the 'standard deviation' of the density of states $n(E)$ as suggested by figure 2. In fact it was implied (Heine 1980) since the 1960s in the Local Moment Method of discussing electronic structure from the point of view of the local atomic environment around an atom (Cyrot-Lackmann 1968, Haydock 1980, Finnis 2003). Here the second moment of the density $n(E)$ of states is a measure of its spread. It is given by the number of out-and-return steps in the Hamiltonian from one atom to its neighbours and back, i.e. is given by Ch^2 in the simplest case of a system with one type of electronic state on each atom. Thus the second moment has dimensions of E^2, and we want a quantity related to the spread in $n(E)$ itself and hence to the cohesive energy as seen in figure 2, i.e. we want the square root of the second moment rather than the second moment itself. This is presumably why the square root result (equation (2)) and its implications do not seem to have been recognised in the early work with the Moment Method. Rather the second moment was used as a first step in fitting some chosen form for $n(E)$, with third and higher moments then adding smaller details (Cyrot-Lackmann 1968, Ducastelle and Cyrot-Lackmann 1970 and 1971).

Clearly the *sp*-bonded metals such as aluminium and zinc do not conform to the restriction to one type of electron only, but Jacobsen et al. (1987) have included the *sp*-bonded metals in a long paper discussed in section 5. It is based on Density Functional Theory (Hohenberg and Kohn 1964, Kohn and Sham 1965) and through several transformations following the variational principle to derive a system of neutral atomic entities with relatively weak interaction between them. While the picture is analogous to ours, the structure of their article is more as a method of calculation. Thus it is that the square root of C is not mentioned directly, but certainly seems inherent in their theory. For example the type of surface reconstruction discussed in connection with figure 7 (section 1) seems to be what is driving their calculated results for the [110] surface of aluminium.

One wonders how far the present concepts are still applicable to elements further to the right of the Periodic Table. Here bismuth has been referred to as a 'semi-metal'. Also yellow phosphorus is rather 'malleable': at least it seemed somewhat soft like a wax candle when one of us (V.H.) in the 1940s watched his elderly school teacher use a pocket knife to cut off a small specimen from a fat stick of it!

It remains to add some historical context, with our present story illustrating "How difficult it is to think a thought that no one in the world has ever thought before!" (Anon). It has certainly taken decades since Bloch (1929) to recognise and integrate the main three themes above, although logically already implied by that work, namely (a) the concept of cluster bonding, and two features (b) and (c) arising from the unusual shape of the $-\sqrt{C}$ function.

Of course chemistry developed historically from the simplest molecules and their understanding in terms of bonding between *pairs of atoms*, which was taken over later in the description of H_2^+ and H_2 etc. with quantum mechanics.

But it is astounding how already Bloch's (1929) paper laid clear foundations for the present work. Firstly he took over from Wigner (1927) the deductive use of group theory to specify mathematically how the one-electron wave functions in a crystalline solid must have the form that we now call Bloch's theorem. Each of them spreads uniformly throughout the whole solid, is labelled by a reduced wave-vector $\mathbf{k}$ in the Brillouin zone, and has its energy in bands $E_n(\mathbf{k})$, with a Fermi energy between the lower filled states and upper empty ones. Secondly Bloch explicitly followed the theory of Heitler and London (1927) for the hydrogen molecule in writing the one-electron Bloch functions to a first approximation as linear combinations of atomic orbitals, (i.e. linear combination of atomic orbitals (LCAO) or 'tight binding' in today's jargon). Moreover in the first four columns of the Periodic Table the Bloch orbital of lowest energy would have $\mathbf{k} = 0$ and show the atomic orbital of one atom in a covalent bonding relationship with that on a neighbouring atom, again as in Heitler and London's treatment of the hydrogen molecule. But note: it is inherent in Bloch's theorem that in a close-packed metallic structure this bonding relationship would apply from one atom equally in the directions to *all* of the neighbours, as shown for example by the actual $\mathbf{k} = 0$ Bloch function in figure 1 computed later by Wigner and Seitz (1933). Thus the concept of *cluster bonding* is mathematically implied by Bloch's theorem, as is the LCAO approximate form of wave function.

An alternative description of the bonding in metals has been given by Pauling, and his two main points certainly seem entirely correct and appropriate (Pauling 1938 and 1949). Firstly the nature of the bonding is analogous to the covalency in the hydrogen molecule, and secondly the bonding is enhanced by the quantum mixing of bond patterns ("chemical resonance") pictured very crudely in figure 3 but discussed mathematically in section 4 (equations (26) and (27)) as a specifically quantum effect, where equation (26) is taken from Pauling (1960, p 12). In particular we also mentioned what the Bloch determinant for the benzene (little metalic ring) molecule becomes when expressed in terms of the 400 arrangements of localised bonds such as those shown in figure 14, not just the two Kekulé ones mentioned by Pauling. It seems that the 'chemical resonance' insight did not lead him to further useful developments regarding metals, because in the Third Edition of his book the index lists 17 references to 'resonance' but none of them to the chapter on metals (Pauling 1960)!

The lowering of the kinetic energy with its role in bonding between neighbours is clear in the LCAO Bloch formulation of a metal wave function, but it appears that it was only in the 1960s that the seeming paradox with the Virial Theorem (see appendix B) was resolved by the detailed calculations of Ruedenberg and co-workers (see Schmidt et al. 2014 a and b). The 1960s were also a time of discussion about the origin of anti-ferromagnetism and nature of the metal-insulator transition, with consideration of what happens if one increases the interatomic spacing of a hydrogen molecule or a cubic crystal of hydrogen atoms slowly without limit (which also resolved the issue of the Virial Theorem as discussed towards the end of appendix B).

The Method of Moments also came in the 1960s for calculating the *local* density of states $n(E)$ on one or more specified atoms of a transition metal such as at a surface (Cyrot-Lackmann 1968). It came as a computational technique, where the first step, namely the second moment, is the 'variance' of the density of states distribution (in the jargon of mathematical statistics) and the square of its 'standard deviation'. This leads directly to the square root form (equation (2)) for the local bonding energy as explained above, although this does not seem to have been used explicitly until some years later as in the 1980 review of the Moment Method (Heine 1980, pp 82-83).

There was no doubt by 1980 about the correctness of the square-root form in equation (2) (for transition metals) from the Mathematical appendix A and the Moment Method, but the square-root is an unusual functional form in physics and one would like a physical picture of its origin in the present context. The only related example in the physics of materials is the expected final distance from the starting point of a random walk of n steps, which in fact provides the clue. The n'th order moment of the density of states is the summed product of the Hamiltonian matrix elements along a returning path of n random steps (Cyrot-Lackmann 1968), and the breadth of the density of states distribution is the square root of the second moment. By now the square root in equation (2) has found its place in the mainstream of electronic structure theory (for example Harrison 1983, Drautz and Pettifor 2006) although unusual in the 1960s and 1970s. See also the discussion towards the end of section 5.

The next stage of understanding came with the empirical modelling of metallic structures initiated by Daw and Baskes (1983, 1984), expressed simply in terms of the *total* number C of neighbours (equation (16)) for both transition and *sp*-bonded metals. Also the square root form (equation (2)) was soon found by Finnis and Sinclair (1984) to 'fit the bill' for their energy function (equation (17)). The unusual curvature of the square root function then gradually rationalised the observations labelled as themes (b) and (c) as mentioned above.

The square root form had only been derived (appendix A) for a metallic band with just one type of electron, to which the transition metals approximated quite well, as remarked before. To test how well one might expect it to apply to *sp-bonded* elements Robertson et al. (1993) in Cambridge carried out the ab initio calculations on 17 structures of aluminium described in sections 1 and 5. The results shown in figure 5 lie surprisingly close to the curve of $-\sqrt{C}$. Not only is the square root the dominant term, but the scatter about it is also not large, coming in the Method of Moments from the third and higher moments of the local density of states.

Actually not known to us in Cambridge, Jacobsen et al. (1987) had already carried understanding a big step forward (see sections 2 and 5), although couched as an improved ab initio calculational method rather than an interpretive discussion. However the two most important points of their work were that it applied equally to both *sp*-bonded and transition metals, and that they proved "The form of the interaction (their equation (7.21)) is identical to the one *assumed* by Daw and Baskes 1983". Several comments by Jacobsen et al. (1987) have a similar ring to our concept of cluster bonding (item 'a' above), including their citing the small energy differences between the three typical crystal structures. Also the significance of their detailed calculations on the structure of the Al [110] surface has already been mentioned above. Finnis (2003, section 8.2) has included an account of their ideas with the comment that the use of the Thomas Fermi approximation for the exchange energy of the electron gas can give a simplified route to the same general end.

Acknowledgments

The authors are hugely greatly indebted to Dr. R.O. (Bob) Jones for encouragement and especially his guidance to the relevant chemical literature. Also, crucial to the thinking in the present work were three visits, all around 1955-1965 by V.H.. One was a visit to the group of Prof. J. Friedel in Paris, learning about formulating quantum calculations about materials in local terms for situations with different atoms having different local situations such as at surfaces. That was the 'Method of Moments' later leading to equation (2). Another was spending two summers as a visitor in the theory group at Harwell, where the problem of modelling radiation damage in metals was an important issue (section 2). Thirdly there was a visit by Prof. J. Friedel to Cambridge during which V.H. heard about the 'Friedel' oscillations of electron density around an impurity in a metal, and was struck by the analogy to the variation of reactivity at the 'ortho', 'meta', and 'para' positions around a benzene ring from an attached side-group. Also formative for V.H. as an undergraduate in New Zealand in the early 1950s were three lectures by the Head of Chemistry, Prof. F.G. Soper, on his return after a sabbatical leave overseas. These lectures (non-examenable!) for senior students introduced quantum mechanics with its applications to chemistry. S.C. acknowledges financial support from the Cambridge Trust and from the Winton Programme for the Physics of Sustainability. Finally, we apologise that in trying to communicate equally with physicists, chemists and material scientists with their different backgrounds, we will have been either too elementary or assumed too much in places for some of them.

Mathematical appendix A

We give here a direct proof that the right-hand side of equation (2) is an exact result for the standard deviation of the density of states distribution in the simplest type of system envisaged in section 1, with the mathematics not embedded in the wider 'Method of Moments' or 'Recursion Method' for calculating the local electronic structure of materials. At issue is the square root in equation (2), somewhat unusual in treatments of electronic structure.

As in section 1 we start with a material consisting of monovalent atoms at a single interatomic spacing with a band of atomic s-electron orbitals only, and hence with a single inter-atomic interaction integral or 'bonding energy' or 'hopping integral' only. We choose the atomic s-electron energy level E_0 as our zero of energy, and use h (negative) for the 'hopping' or 'bonding' integral between neighbouring atoms. The Hamiltonian matrix H for the electronic structure then looks something like

$$H_{ij} = \begin{pmatrix} 0 & h & 0 & h & h & \cdot & \cdot & \cdot \\ h & 0 & h & 0 & 0 & & & \\ 0 & h & 0 & 0 & h & & & \\ h & 0 & 0 & 0 & h & & & \\ h & 0 & h & h & 0 & & & \\ \cdot & & & & & \cdot & & \\ \cdot & & & & & & \cdot & \\ \cdot & & & & & & & \cdot \end{pmatrix} . \tag{32}$$

We will need to consider the matrix H^2 written in two different representations. The first is the atomic representation, the same as in equation (A.1). In fact we shall only need the diagonal matrix elements of H^2 which are, when equation (A.1) is squared,

$$[H^2]_{ii} = \sum_j H_{ij} H_{ji} C_i h^2, \tag{33}$$

where C_i is the 'coordination number' of atoms j neighbouring to atom i. The second representation of H^2 is in terms of the eigenfunctions of H, i.e. we have

$$[H^2]_{nn} = E_n^2 \tag{34}$$

with E_n the n'th largest eigenvalue of H.

The two matrix forms of the 'operator' H^2 in equations (A.2) and (A.3), called the 'trace', are related in matrix theory by a 'unitary transformation', and by a standard matrix theorem the sums of the diagonal elements (equations (A.2) and (A.3)) are equal when summed over all the atoms i in equation (A.2) and eigenstates n in equation (A.3) (Mathews and Walker 1965, equations (6.54) and (6.56)).

We now have to interpret the traces of equations (A.2) and (A.3) when summed. Let us first consider a specimen in the form of a perfect crystal of N atoms all having the same coordination number C of neighbours around each atom. Then equation (A.2) summed becomes

$$\text{Trace}[H^2] = NCh^2, \tag{35}$$

whereas equation (A.3) summed is

$$\mathrm{Trace}[H^2] = \sum E_n^2 = N w_{\mathrm{rms}}^2, \tag{36}$$

where w_{rms} is the 'root mean square' band width of the distribution of energy eigenvalues E_n in the sense of the density of states in figure 2. When the coordination number C is the same for all atoms we can drop the factor N and write from equations (A.4) and (A.5)

$$w_{\mathrm{rms}}^2 = Ch^2, \tag{37}$$

As argued in section 1 the bonding energy per electron-per-atom is roughly

$$w_{\mathrm{rms}} = \sqrt{C}|h|, \tag{38}$$

and we can extend this by writing

$$w_{\mathrm{rms}}(\text{at atom } i) = \sqrt{C_i}|h|, \tag{39}$$

for situations where not all the atoms are equivalent, e.g. at a surface. Equations (A.6) to (A.8) can be generalised similarly when not all atoms are at the same interatomic spacing or indeed of the same chemical element.

It remains to prove equation (A.6) for a pure d-band as a good approximation for a transition metal. Each non-zero element H_{ij} of the Hamiltonian matrix (equation (A.1)) between nearest neighbour atoms i and j becomes a little 5×5 matrix for the five atomic d-orbitals on those atoms. For each such pair of nearest neighbours i and j we can make a unitary transformation to make the direction joining the pair as the local z-axis, and the matrix elements between them then become the $dd\sigma$, $dd\pi$ and $dd\delta$ hopping matrix elements. Thus for each pair of nearest neighbours the h^2 in equation (A.6) becomes (Ducastelle and Cyrot-Lackmann 1970 and 1971)

$$(dd\sigma)^2 + 2(dd\pi)^2 + 2(dd\delta)^2, \tag{40}$$

with corresponding changes in equations (A.7) and (A.8) as discussed in section 1.

The theory can in fact be extended even further to cover a NFE metal such as aluminium with a conduction band that is a mixture of $3s$ and $3p$ states (or to include both the s and d states of a transition metal). However the result and proof become more complicated as described at the end of section 5 without a full mathematical discussion.

Mathematical appendix B: The Virial Theorem in relation to kinetic energy in covalent bonding

The Virial Theorem is a mathematical result concerning the kinetic and potential energies T and V of a set of mobile particles, interacting with each other and with fixed centres, with a repulsive or attractive potential proportional to r^n where n is a positive or negative integer. The treatment may be by algebra or differential equation, classical or quantum mechanical. The best known example is of course simple harmonic motion for $n = 2$ where T and V are each equal to half of the total energy E.

The situation of interest here is that of $n = -1$, i.e. Coulombic interactions (Fock 1930), and specifically for the discussion of covalent bonding we choose for simplicity the hydrogen molecular ion H_2^+ with one mobile electron interacting with two fixed protons spaced a distance a apart. In this case the Virial Theorem states that

$$V = -2|E| \qquad (V \text{ and } E \text{ both negative}) \tag{41}$$

$$\text{and} \qquad T = |E|. \tag{42}$$

If we choose the inter-proton distance a to be very large, we effectively have one neutral hydrogen atom plus one bare proton far away from it, and the total energy E is simply -1 Rydberg, the ground state energy of an electron in the 1s state of a hydrogen atom. However we know that in reality the hydrogen molecular ion is a stable bonded system, so that if we consider the bare proton to be drawn into the region of the (other-proton + electron) sub-system there will be a decrease in total energy E, i.e. the hydrogen molecular ion is more tightly bound than the hydrogen atom. Figure 15 shows a qualitative sketch of the molecular orbital in the hydrogen molecular ion (full line), and for comparison an atomic $1s$ wave function sketched around each proton. It shows that the molecular orbital is much flatter in the region between the two protons, which in quantum mechanics represents a lower kinetic energy of the electron there, as has been verified by the computations by Schmidt et al. (2014).

Indeed this lowering of the kinetic energy in the bond is generally accepted as characteristic of covalent bonding: see particularly the reference Schmidt et al. 2014 (a and b). However the virial result (equations (B.1) and (B.2)) now presents us with a seeming contradiction: as the (negative) E has gone more negative, the total kinetic energy from equation (B.2) has had to have gone up! The latter effect can indeed be seen in figure 15 in the outer regions of the wave function where the lowering of the electron energy results in a steeper drop of the wave function $\psi(\mathbf{r})$ at large $|\mathbf{r}|$. That steeper drop of course represents an increase in kinetic energy there in accordance with equation (B.2), but it also locates the electron in closer to the two protons, and thus contributes to a lowering of the potential energy.

In conclusion, we can see four effects in the hydrogen molecular ion (and which are present in covalent bonding generally). Firstly the flatness of the wave function between the two protons represents a reduction of kinetic energy there. Secondly the build-up of electron density there gives locally a larger (more negative) potential energy. Thirdly in the outer region of the hydrogen molecular ion, the wave function ψ drops off more strongly as $|\mathbf{r}|$ tends to infinity, i.e. the wave function has been pulled inwards towards the two protons, which gives a further lowering of the electron's potential energy. Finally that pulling in of the wave function and consequent greater steepness for large $|\mathbf{r}|$ results in a higher kinetic energy there. Of these four effects, it might be too anthropomorphic to describe the flatness of the wave function between the two protons as driving the net bonding, but one could perhaps call that its 'signature tune'. It applies not only to the hydrogen molecular ion, but is of the essence where atomic orbital spread out towards neighbours in any type of covalent bonding (Schmidt et al. 2014a).

References

L. C. Allen and J. K. Burdett, Angew. Chemie Int. Ed. Engl. 34, 2003 (1995)

N.W. Ashcroft and N.D. Mermin, Solid State Physics. Holt, Rinehart and Winston, New York (1976).

F. Bloch, Z. Phys. 52, 555 (1929).

D.W. Bullet, Solid State Phys. 35, 129-214 (1980).

F. Cyrot-Lackmann, J. Phys. Chem. Solids, 29, 1235-1243 (1968).

M. S. Daw, Phys. Rev. B 39, 7441-7452 (1989).

M. S. Daw and M. I. Baskes, Phys. Rev. Lett. 50, 1285 (1983).

M. S. Daw and M.I. Baskes, Phys. Rev. B 29, 6443-6453 (1984).

R. Drautz and D.G. Pettifor, Phys. Rev. B74, 174117 (2006).

F. Ducastelle and F. Cyrot-Lackmann, J. Phys. Chem. Solids 31, 1295-1306 (1970).

F. Ducastelle and F. Cyrot-Lackmann, J. Phys. Chem. Solids 32, 285-301 (1971).

M.W. Finnis, Interatomic Forces in Condensed Matter. Oxford University Press (2003).

M.W. Finnis and J.E. Sinclair, Philos. Mag. A 50, 45 (1984).

V. Fock, Zeits. F. Physik 63, 855-858 (1930).

S.M. Foiles, J. Materials Research 4, 102-112 (1989).

J. Friedel, Adv. in Phys. 3, 446 (1954).

W.A. Harrison, Phys. Rev. B 27, 3592-3604 (1983)

R. Haydock, Solid State Phys. 35, 215-294 (1980).

V. Heine, Introduction to the Use of Group Theory in Quantum Mechanics. Pergamon Press (1960). Reprinted by Dover, New York (2007).

V. Heine, Solid State Phys. 35, 1-127 (1980).

W. Heisenberg, Zeits. D. Physik 39, 499 (1926).

W. Heitler and F. London, Zeits. F. Phys. 44, 455 (1927).

P. Hohenberg and W. Kohn, Phys. Rev. 136, B864-871 (1964).

K. W. Jacobsen, J. K. Nørskov, and M. J. Puska, Phys. Rev. B 35, 7423 (1987).

R.O. Jones, J. Chem. Phys. 99, 1194-1206 (1993).

R.O. Jones, J. Phys.: Condens. Matter 30, 153001 (2018).

R.O. Jones, J. Phys.: Condens. Matter 34, 343001 (2022).

M.J. Kelly, Solid State Phys. 35, 295-382 (1980).

W. Kohn and L. Sham Phys. Rev. 140, A1133 (1965).

J. Mathews and R.L. Walker, Mathematical Methods of Physics. Benjamin, (1961).

N.F. Mott and H. Jones, The Theory of the Properties of Metals and Alloys. Clarendon Press, Oxford (1936). Reprinted by Dover, New York (1958).

L. Pauling, Phys. Rev. 44, 899 (1938).

L. Pauling, Proc. Roy. Soc. A196 343-362 (1949).

L. Pauling, The Nature of the Chemical Bond. Cornell Univ. Press (1960).

I.J. Robertson, V. Heine and M.C. Payne, Phys. Rev. Lett. 70, 1944 (1993).

A. Savin, O. Jepsen, J. Flad, O.K. Anderson, H. Preuss and H.G. von Schnering, Angew. Chemie Int. Ed. Engl. 31, 187-188 (1992)

M.W. Schmidt, J. Ivanic, and K. Ruedenberg, (a) J. Chem. Phys. 140, 204104-1 (2014).

M.W. Schmidt, J. Ivanic, and K. Ruedenberg, (b) The Chemical Bond: Fundamental Aspects of Chemical Bonding, edited by G. Frenking and S. Shaik. John Wiley & Sons, (2014).

E. Schrödinger, Proc. Camb. Phil. Soc. 31, 555-563 (1935).

B. Silvi and C. Gatti, J. Phys. Chem. 104, 947-953 (2000)

A.P. Sutton, M.W. Finnis, D. G. Pettifor and Y. Ohta, J. Phys. C: Solid State Phys. 21, 35-66 (1988).

E. Wigner, Zeits. F. Phys. 43, 624 (1927).

E. Wigner and F. Seitz, Phys. Rev. 43, 804 (1933).

J.M. Ziman, Principles of the Theory of Solids. Cambridge University Press (1964).

Figures

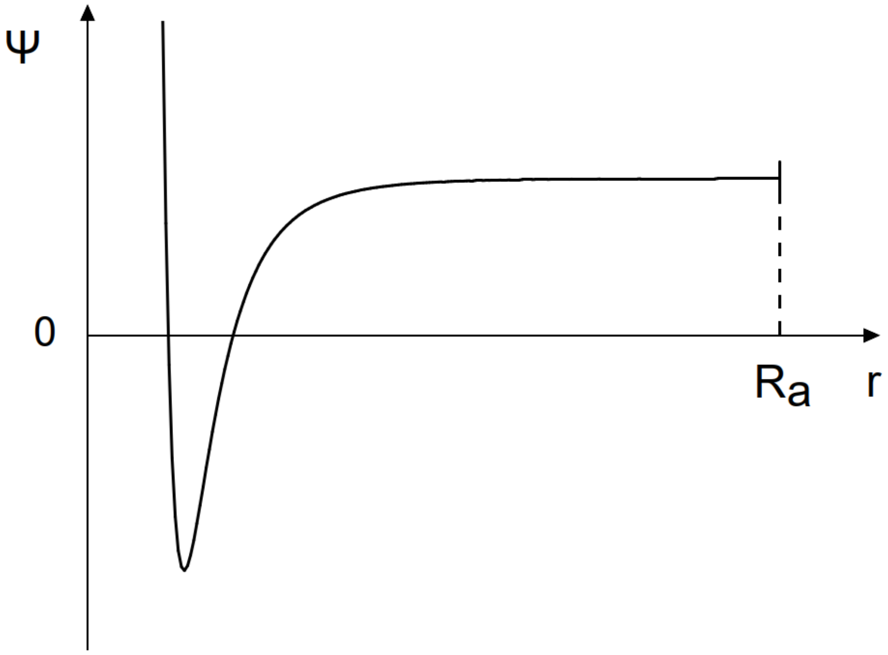

Figure 1. Radial wave function for sodium metal as calculated by Wigner and Seitz (1933) at an energy giving zero gradient at the radius of an atomic sphere. This approximates very closely to the energy and wave function at the bottom of the conduction band.

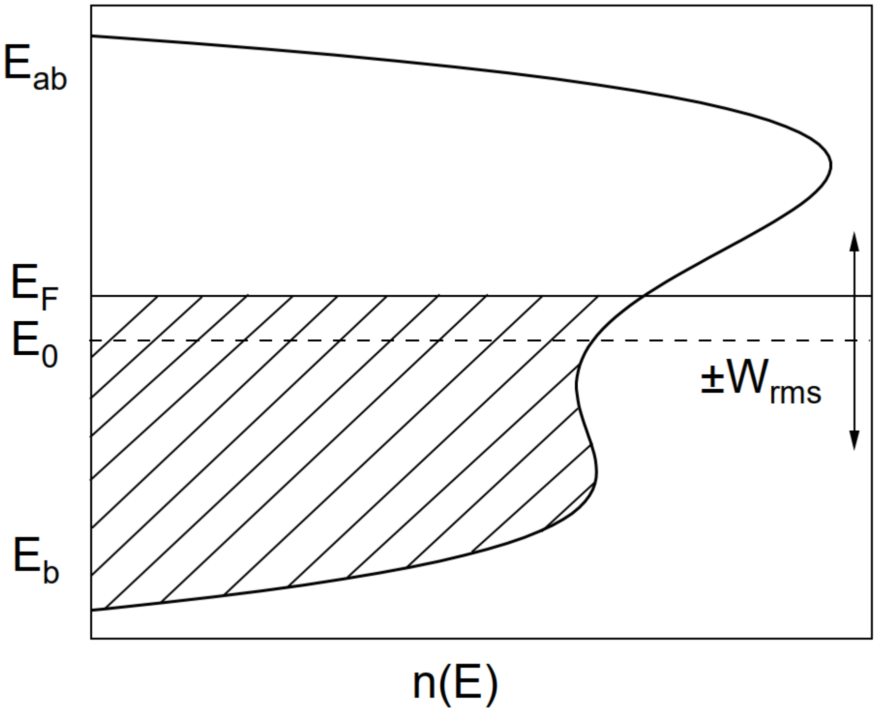

Figure 2. The energy density of states $n(E)$ in the conduction band of a hypothetical metal having only one s-electron per atom, shown as a function of the energy E between the totally bonding and totally antibonding states at energies E_b and E_{ab} respectively (schematic). All the states are filled with energies below the Fermi level E_F. Note the root-mean-square breadth of the distribution W_{rms} around the band's central energy E_0.

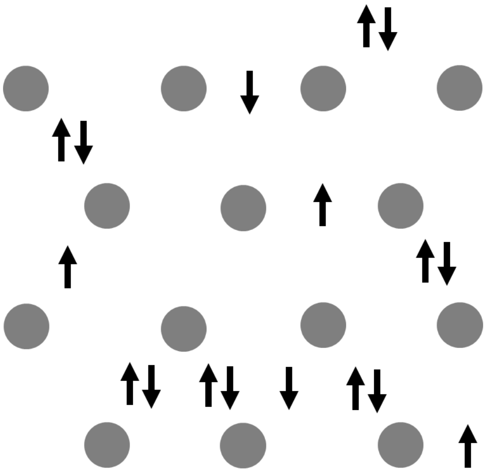

Figure 3. The quantum state of lowest energy (ground state) of a metal contains within it all possible arrangements of up and down spin electrons between neighbouring atoms such as in the snap-shot envisaged here, in permanent ‘reverberation’ or ‘chemical resonance’ among them.

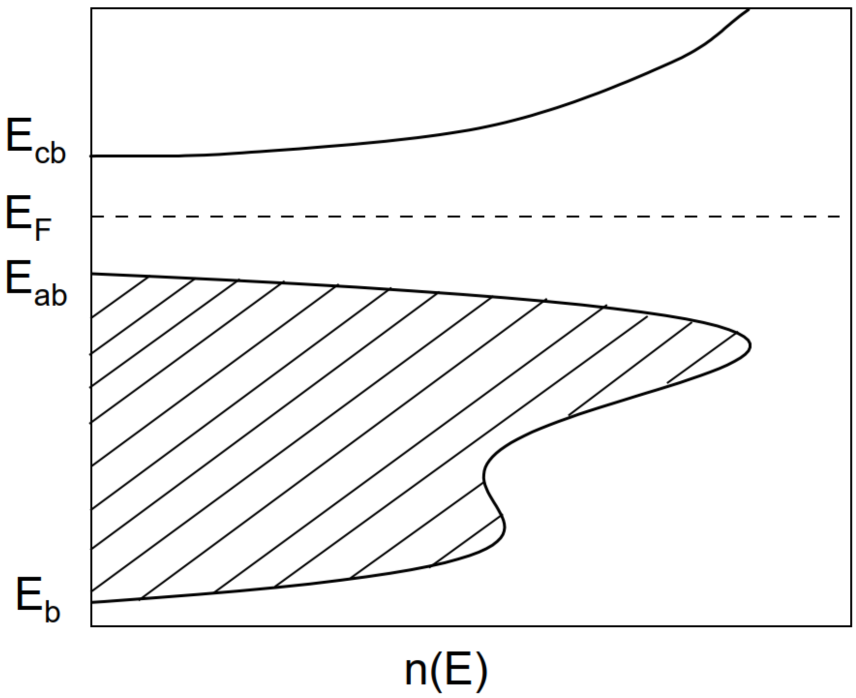

Figure 4. Electronic density of states $n(E)$ (schematic) for diamond, with a completely filled 'valence' band and a totally empty conduction band, with Fermi level lying in the substantial energy gap in between.

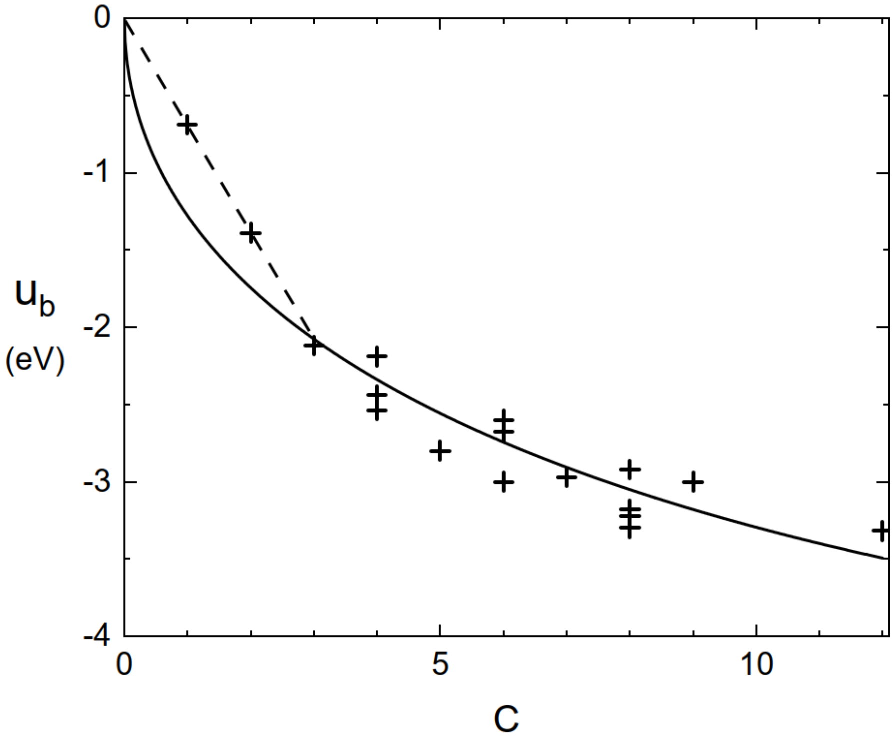

Figure 5. Computed ab initio energies (per atom) of 17 structures of aluminium ranging from $C = 1$ (free dimer molecule) to $C = 12$ (face-centred cubic crystal). (After Robertson et al. (1993)). Note the closeness of the calculated points about the square root curve (full line), with a very modest scatter about it representing contribution from higher moments of the density of states.

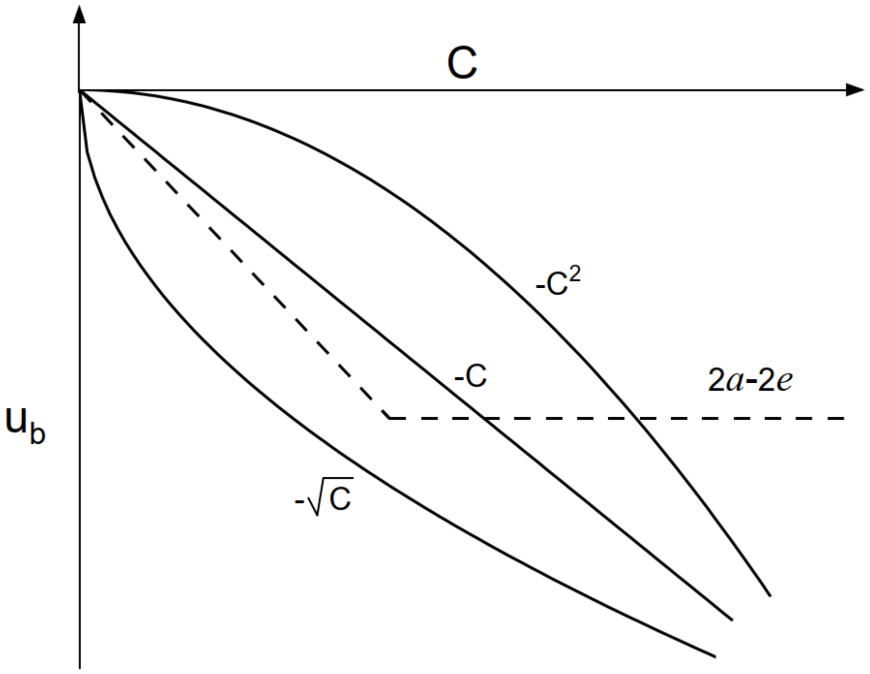

Figure 6. Four algebraic forms for how the bonding energy might conceivably vary with the coordination number C for atoms involving one type of orbital only. The dashed line represents all that is possible with 'two-atom two-electron' covalent bonds. Energies from 3-atom interaction including bond angle effects would give a quadratic contribution varying as $-C^2$ to the total energy which has completely the wrong shape as shown.

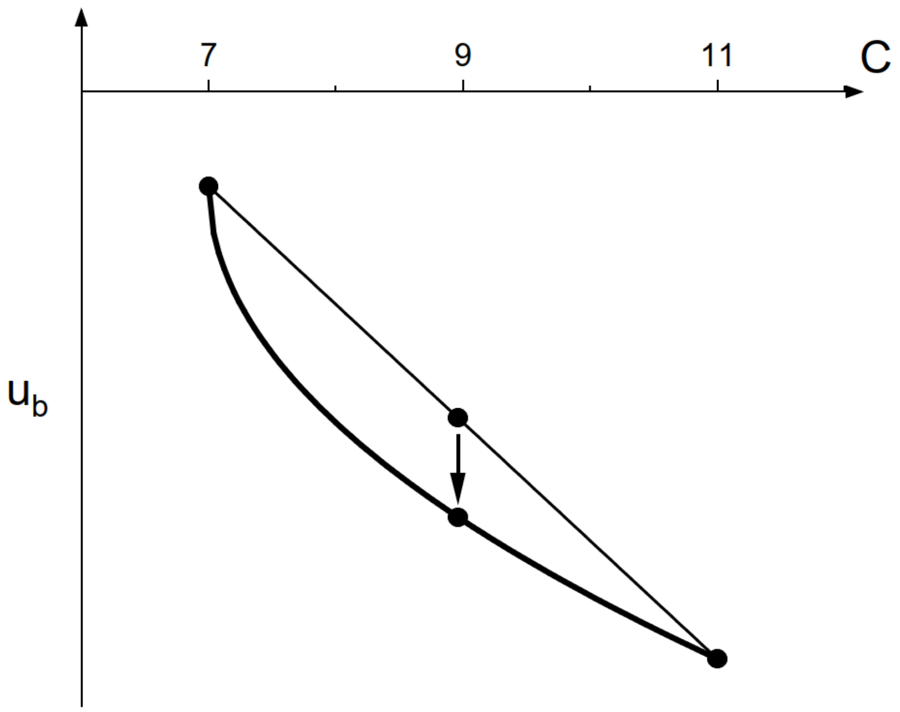

Figure 7. The upward curvature of the square root function can drive surface reconstruction from a rough bare open surface with two partial layers of 7- and 11-coordinated atoms, to one type of layer with all $C = 9$.

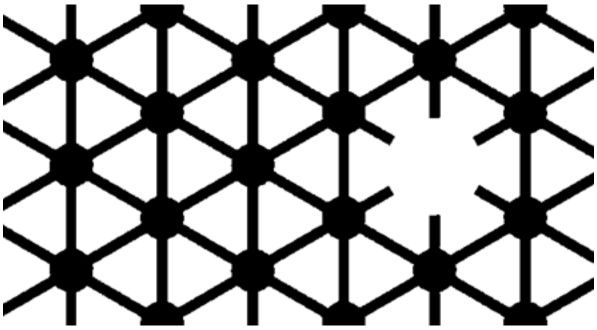

Figure 8. Bonding in a fcc metal, in the bulk metal on the left and around a vacancy on the right.

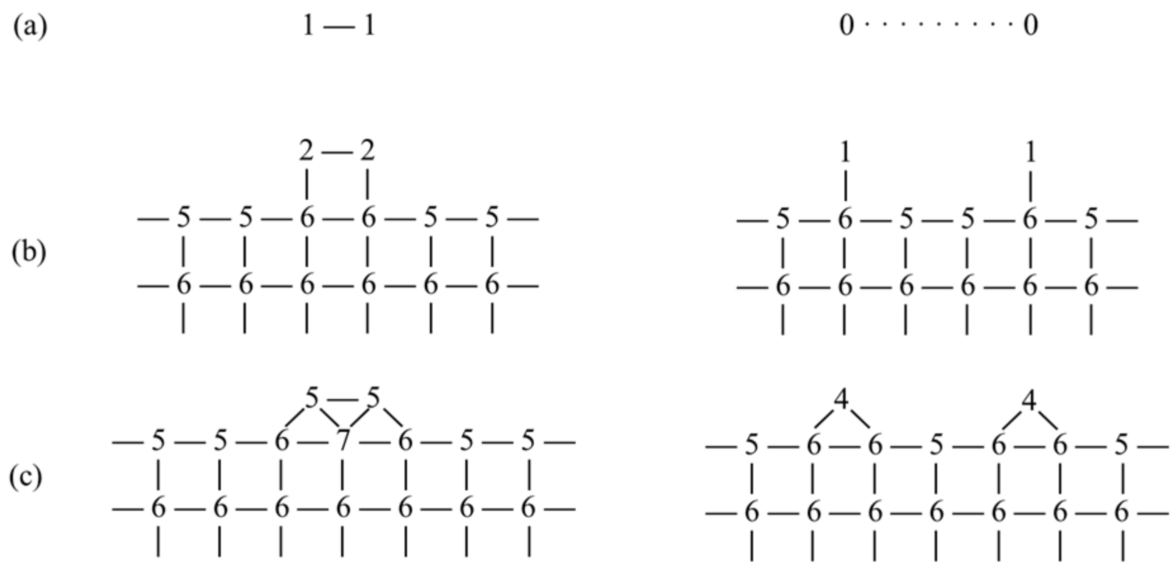

Figure 9. The number of bonds at each atom of a metal dimer molecule, on the left as an intact molecule and on the right when dissociated. (a) As the free molecule. (b) With the molecule adsorbed on top of bulk atoms of a [100] surface of the same metal, the equilibrium interatomic spacing being assumed to be the same as that of the bulk metal. (c) Analogue to (b), applied to two adjacent atomic layers but with the adsorption sites above the centres of surface atomic squares on two adjacent atomic layers.

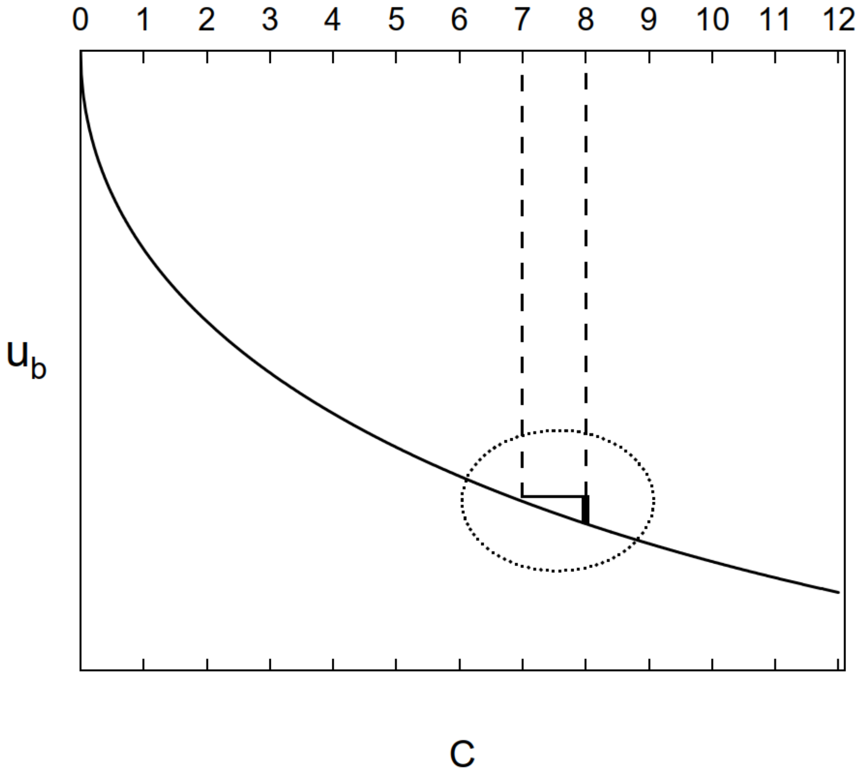

Figure 10. The small energy cost when a dimer molecule dissociates while adsorbed on the surface of some material. The coordination number of each atom of the molecule is reduced from, say, $C = 8$ to $C = 7$ when on the surface, compared with going from $C = 1$ to $C = 0$ as a free molecule in the gas phase. The curve shown has the square root form of equation (2).

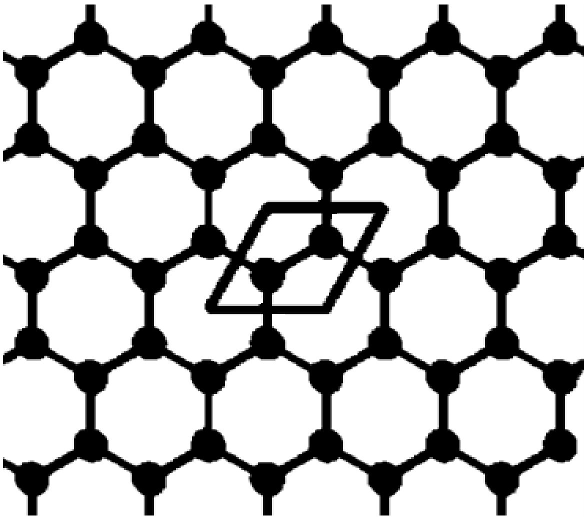

Figure 11. The hexagonal net of carbon atoms in a single atomic layer of graphite, with the crystallographic unit cell shown.

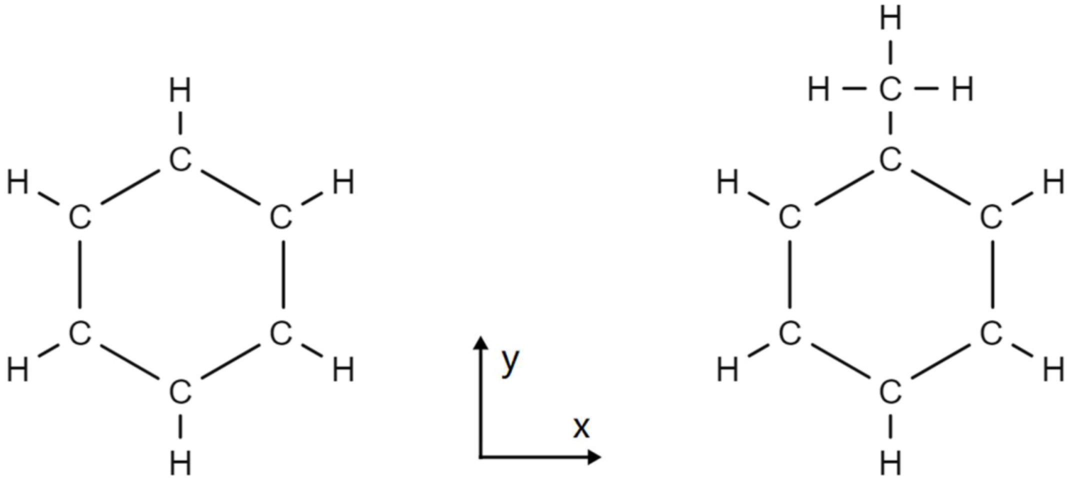

Figure 12. The structure of (left) the benzene molecule C_6H_6 and (right) toluene C_6H_5-CH_3. The bonds shown are only the σ-bonds in the xy plane.

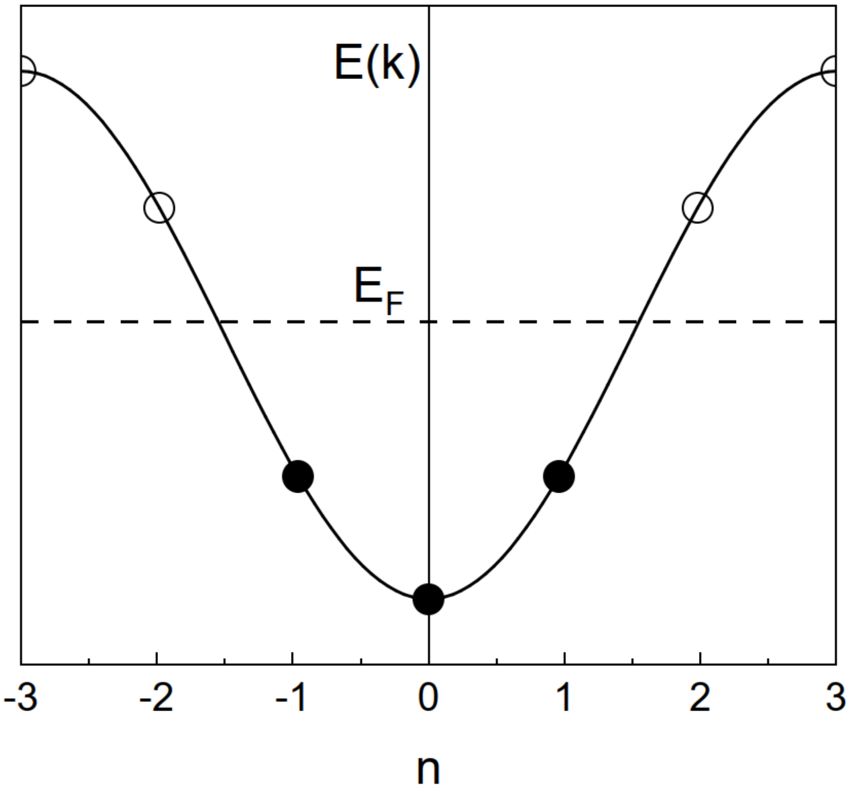

Figure 13. Energies $E(k_n)$ of the molecular orbitals of the $2p_z$ π-electrons, with the k_n of equations (24) and (25).

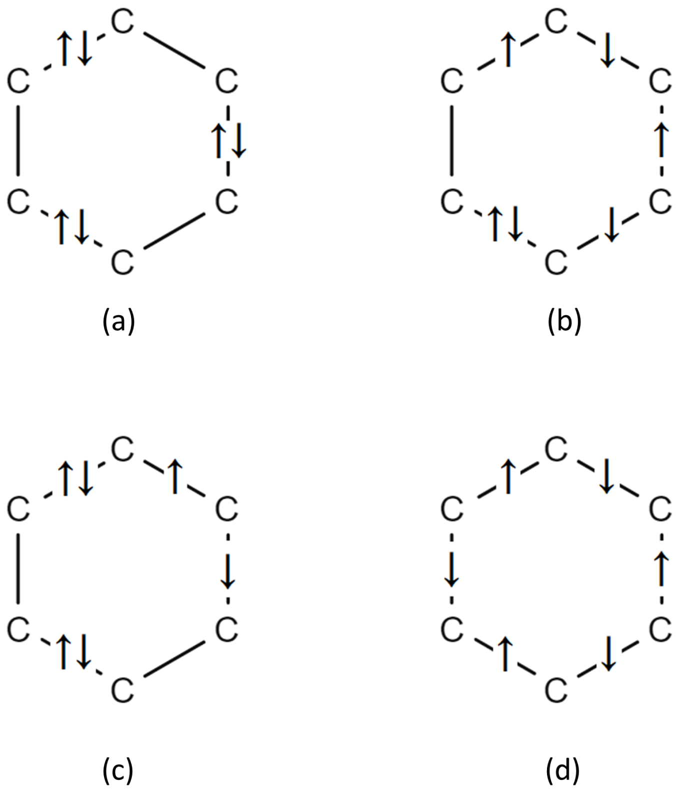

Figure 14. Four of the possible ways (out of 400) of distributing the six $2p$ π-electrons in bonding orbitals between neighbouring carbon atoms. Of these (a) is one of the two Kekulé structures, and (d) has the electronic charges and spins spread out as much as possible.

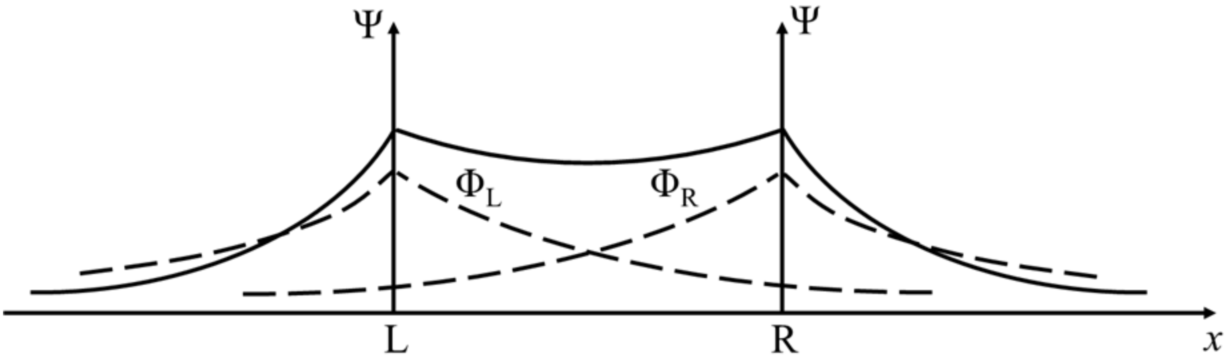

Figure 15. The bonding molecular orbital (schematic) of the hydrogen molecule (heavy line) with a flattened filled-in shape along the x-axis between the two hydrogen atom nuclei, and a more rapid drop-off beyond them. Atomic $1s$ orbitals Φ around the two nuclei are shown dashed (to a smaller scale).